Preparation and characterization of DNA-Gold nanocomposites for metal ion detection

A dissertation report submitted in partial fulfilment of the requirement for the award of degree of

Master of Technology in Biotechnology

Submitted by

Khyati Rana

601204013

Under the supervision of:

Dr. Niranjan Das
Professor
Department of Biotechnology

Dr. Bonamali Pal
Professor & Head
School of Chemistry & Biochemistry

THAPAR UNIVERSITY
PATIALA

CERTIFICATE

This is to certify that the report entitled "Preparation and characterization of DNA-Gold nanoparticles for metal detection" submitted by Khyati Rana in partial fulfilment of the requirement for the award of Degree of Masters in Technology in Biotechnology to Thapar University, Patiala, is a record of student's own work carried out by her under my supervision and guidance. The report has not been submitted for the award of any other degree or certificate in this or any other university.

Dr. Niranjan Das
Professor
Department of Biotechnology

Dr. Bonamali Pal
Professor & Head
School of Chemistry & Biochemistry

Dr. Dinesh Goyal
Head of Department
Department of Biotechnology
Thapar University, Patiala

Dr. S.K. Mahopatra
Dean (Academic Affairs)
Thapar University, Patiala

CANDIDATE'S DECLARATION

I hereby declare that the work being presented in the report entitled "Preparation and characterization of DNA - Gold nanoparticles for metal detection" in partial fulfilment of the requirement for the award of Degree of Masters in Technology in Biotechnology to Thapar University, Patiala is my own work during the period of July 2013 to June 2014, under the supervision of Dr. Niranjan Das, Professor, Department of Biotechnology and Dr. Bonamali Pal, Professor & Head, School of Chemistry & Biochemistry, Thapar University, Patiala. I have not submitted the matter embodied in this report for the award of any other degree.

Khyati Rana

Date: 07/07/2014

Khyati Rana
Roll No. 601204013

It is certified that the above statement made by the student is correct to the best of my knowledge and belief.

Dr. Niranjan Das
Professor
Department of Biotechnology

Dr. Bonamali Pal
Professor & Head
School of Chemistry & Biochemistry

ACKNOWLEDGEMENT

I would like to convey my sincere gratitude to my research guides Dr. Niranjan Das, Professor, Department of Biotechnology and Dr. Bonamali Pal, Professor & Head, School of Chemistry & Biochemistry for their guidance and suggestions which helped me immensely during this course. I am extremely obliged to them for giving me such an innovative and current research topic.

I acknowledge Dr. Smarat Mukhopadhyay, Associate Professor and Ms. Shikha, Lab Assistant, Department of Biotechnology, Indian Institute of Science Education and Research (IISER), Mohali for analysing samples through CD spectrometer.

I express my humble gratitude to Dr. B. K. Chudasama and Ms Navjot, School of Physics and Material Science, Thapar University for measuring Zeta potential and DLA particle size distribution.

I am sincerely thankful to Dr. Satnam and Mr.Inder for FTIR analysis and Dr. Rajesh for permitting to use fluorescence spectrometer.

I heartedly express my sincere thanks to Ms. Rupinder Kaur, Ph.D. scholar, whose help, stimulating suggestions and encouragement helped me in all the time of research and writing of this thesis.

I am obliged to Mr Rohit, Ms Anila, Mr Bhupender (Ph.D. scholars, School of Chemistry & Biochemistry) and Mrs. Dakshi, Mr. Rajneesh, Mr. Lakhvinder (Ph.D. scholars, Department of Biotechnology) for their kind cooperation and support which make my work easier and enjoyable.

I am very thankful to Dr. Dinesh Goyal, Head, Department of Biotechnology, Thapar University for his immense concern throughout the project work.

I am highly indebted to my loving parents for their inspirations, blessings, and financial support.

God grace has kept me on the path of success and helped me in completion of this project.

Date: Khyati Rana

Place: Thapar University

Patiala

List of Contents

Abstract

In present study, Gold nanoparticles of various sizes and shape has been synthesized and coupled with DNA to study the modification in the optical and electrokinetic behaviour. DNA does not show any absorbance in the visible region, but on binding with DNA, a red shift in gold nanoparticles (524 nm to 638 nm) has been observed. TEM shape and size analysis also prove the linking of DNA on Au nanostructures. Change in nanoparticle size distribution from 33 nm to 78 nm due to formation of nanocomposite was calculated through DLS. AFM studies help in correlating various 3D structures of Gold-DNA nanocomposites. Results have shown that fluorescence intensity of DNA increases on binding with gold nanospheres. Using this property, they are used as a low-cost sensing system which is simple and fast for detection of Mg^{+} ions. This sensing system has unprecedented sensitivity with a limit of detection from 20 ppm to 100 ppm for Mg^{+} ions. The fluorescence response of DNA-Gold nanoparticles is remarkably specific for Mg^{+} ions in the presence of other metal ions. This method of sensing is simple and easy to use just by mixing and incubation of the sample for 15 min at room temperature. It has successfully carried out the detection of Mg^{+} ions present in laboratory water and gelusil (an antacid). The DNA-Gold nanocomposite sensing system described here shows promising future potentials in the field of metal ion detection.

1. Introduction

Deoxyribonucleic acid (DNA) is a complex biomolecule that contains all the information required for the maintenance and growth of an organism. It acts as the basic unit of heredity in all types of organisms (Chang et al. 1997). It is a nucleic acid and comprises of three components: a nitrogenous base, a pentose sugar and a phosphate as shown in Figure 1. It consists of two purine bases namely, adenine (A) and guanine (G), and two pyrimidine bases that are cytosine (C) and thymine (T).

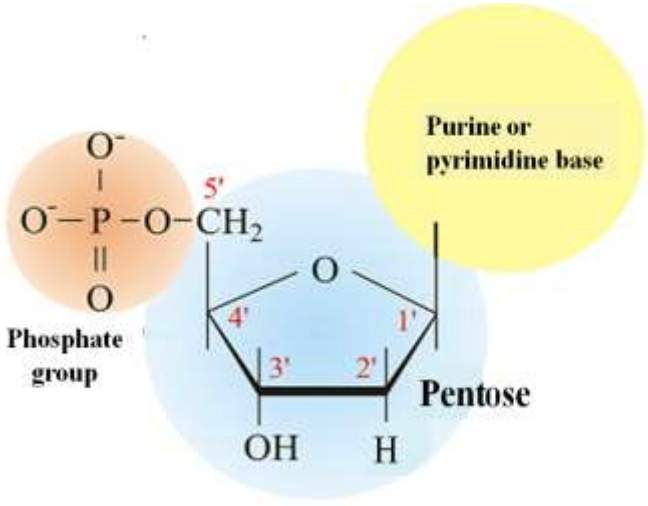

Figure 1. General structure of Deoxyribonucleotide

The numbering of carbon and nitrogen is done in such a way that it facilitates the identification and naming of the derivative compounds. The carbon present in nucleotides is designated by a prime (′) to differentiate them from the numbering of nitrogenous bases. There is N-β-glycosyl covalent bond between nucleotide base (at N-1 of pyrimidines and N-9 of purines) and 1′ carbon of pentose. This bond is formed by the removal of water molecule i.e., a hydroxyl group from pentose and hydrogen from the base. The ester bond is formed by joining the phosphate to 5′ carbon of nucleotide (Friedbreg et al. 1995). The consecutive nucleotides of DNA are bonded by phosphodiester linkage, in which 5′- phosphate group of one nucleotide is joined to 3′ - hydroxyl group of the next nucleotide.

Mostly DNA molecules are double-stranded and helical in shape, consisting of two long strands of nucleotides. These two helical strands run in opposite directions and are anti-parallel to each other, one backbone being 3′ and the other 5′, referring the direction of the 3rd and 5th carbon on the pentose sugar as shown in Figure 2. One of the four types of nucleotides is attached by each and every deoxyribose sugar present in two helical DNA chain (Kamenetskii et al. 1997). In a helix, there is a hydrophilic backbone which is made up of alternating deoxyribose and phosphate groups and these groups are located outside the double helix, facing towards water. The purine and pyrimidine bases are hydrophobic and stacked inside the helix. Due to the hydrogen bonding between bases present on two strands,

a major and minor groove on its surface are created. According to Chargaff's rule, G makes three hydrogen bonds with C and A makes two hydrogen bonds with T. It is the sequence of these four nucleotides along the backbone that encodes the biological information (Olby et al. 1994).

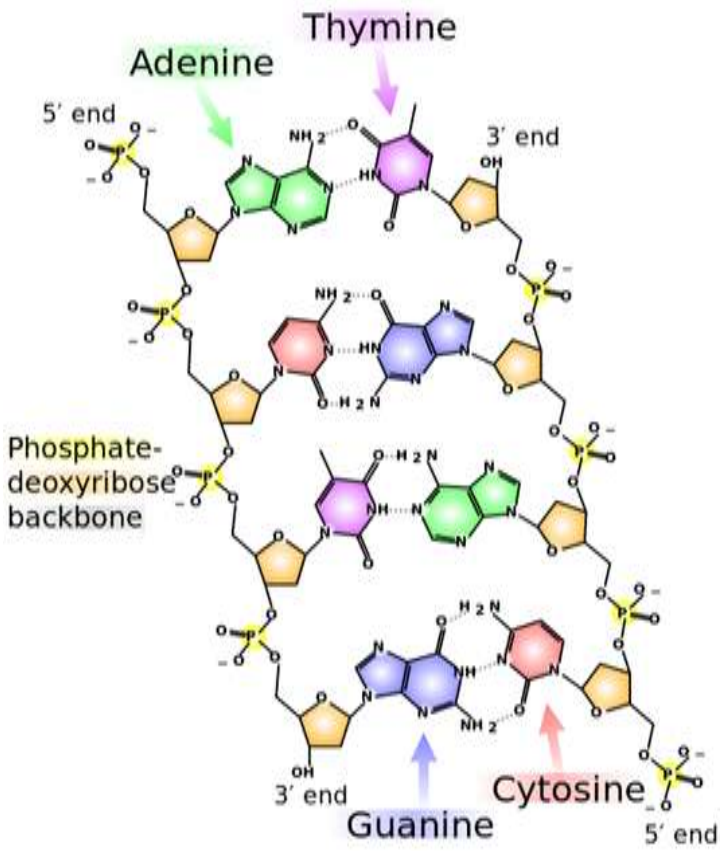

Figure 2. Double stranded DNA showing Watson-Crick base pairing.

In single stranded DNA, the individual repeating unit is the nucleotide. It is more flexible than double stranded DNA, as free rotation is allowed around phosphodiester backbone which is responsible for joining adjacent nucleotides. Single stranded DNA is considered as an electronegative polymer. Electropositive biomolecules and metals commonly take advantage of this electronegative character and bind on its surfaces. Another component available for binding is a nucleotide base itself (Shamoo et al. 2002).

These biophysical properties of DNA make it more useful in the field of applied research. Its compatibility with metals has a variety of applications in biosensor development. Mostly Gold is preferred over other metals because of its uniformity and interesting optical properties. By exploiting these properties, Gold nanoparticles (AuNP) can be used for highly sensitive detection of biomolecules and metal ions. Aggregation of AuNP leads to slight changes in their optical properties which can be detected by shift in the plasmon resonance peak i.e., a red shift and change in colour from red to blue. The surface plasmon resonance of AuNP results from collective oscillation of conducting electrons on interaction with electromagnetic radiation (Cao et al. 2011).

The importance of DNA-modified AuNP can be recognized in the field of biosensing. The unique optical and chemical properties of colloidal gold enhance its use in research. They can

be stabilized with a wide variety of molecules because of alkyl thiol adsorption phenomena. Also, in DNA the specific base pairing and the availability of free hydroxyl and phosphate groups have been used to build structured assemblies of particles (Li et al. 2009). Due to these properties, DNA-functionalized Au nanoparticles are widely used as (Lin et al. 2009):

- Nanoscale building blocks in assembly strategies
- Due to surface Raman scattering of adsorbed molecules, can be used as the substrate of Raman probe design.
- Used as antisense agents in nanotherapeutics
- Probes in many diagnostic systems
- Dynamic compound in photothermal therapy, biosensing, molecular imaging, and gene delivery
- Real-time observable nodes for imaging studies

In the last few decades, the various aspects of advanced research on DNA-AuNP such as synthesis of different shape and sizes of AuNP, their interaction with biomolecules, binding of DNA with different metal ions and studies on the properties of DNA-Au nanocomposites are discussed in the following section, 'Literature Review'.

2. Literature Review

In early 1970's, the independent studies on AuNP and DNA were started. It was for the first time in 1973 when Inagaki et al. studied the optical constants and dielectric properties of calf thymus DNA in the presence of ultraviolet rays. In initial years, more emphasis was given on the correlation between optical properties and morphology of DNA at the molecular level. The studies on synthesis and properties of Au nanoparticles were initiated by Mirkin et al. (1996). The detailed studies on biophysical properties of DNA, DNA-metal interactions, methods of AuNP synthesis, preparation and properties of DNA-Gold nanocomposite and application of DNA-gold nanocomposite in different areas are described in the following sections.

Studies on biophysical properties of DNA: Many researchers studied the conformational changes in DNA in the presence of different variables such as temperature, pH etc. Tomas Lindal (1993) discussed the changes in optical properties due to instability and denaturation of basic DNA structure in his review article. Dorfman et al. (2012) studied the various properties of DNA like DNA stretching, fluorescence, microfluidic separation and burst analysis apart from gel electrophoresis. DNA fingerprinting and barcoding was done to gather more and more genomic information from the DNA. They have also studied the optical properties of DNA.

Different methods of AuNP synthesis: Research on AuNP was started when Mirkin et al. (1996) described the methods for the synthesis of AuNP. They have also given the protocols for synthesis of different shapes of nanoparticles like nanospheres and nanorods. Since then, many studies and experiments have been carried out to explore the more properties of AuNP.

Jana et al. (2001) prepared the gold nanorods with different aspect ratios i.e. 4.6 ±1.2, 13 ± 2, and 18 ± 2.5 in the presence of an aqueous miceller template by a seeding growth method. Citrate-capped 3.5 nm diameter gold particles were used as the seed, prepared by the reduction of chloroauric acid ($HAuCl_4$) with borohydride. They controlled the aspect ratios of the nanorods by varying the ratio of seed to metal salt. The long nanorods were separated from nanospherical particles by centrifugation.

Liang et al. (2007) have developed a centrifugation based method for preparation of AuNP. The nanoparticles produced by this method were a two-step approach i.e. chemical reduction at low concentrations and followed by centrifugation. The AuNP of high concentration were

prepared by this method. It led to AuNP with high salt resistance and high stability, which were useful for preparation of DNA-AuNP composite for DNA biodetection.

Salient properties of AuNP: Pedersen et al. (2005) explained the surface plasmon resonance (SPR) properties of AuNP-coated substrates and with the help of SPR approach they tried to detect some of the reagents like formaldehyde, paraoxon and 2-chloroethyl ethyl sulfide. Li et al. (2005) revealed unique and new optical properties with respect to increased fluorescence of gold nanorods and this was used for detection studies based on monitoring the intensity of fluorescence of gold nanorods (AuNR).

Liao et al. (2005) stabilized the gold nanorods (AuNR) in the absence of CTAB surfactant by making the use of thiol terminated methoxypoly (ethylene glycol) so that nanorods remained stable in buffer solution. These nanorods were then combined with immunoglobulin G (IgG) antibodies which lead to the formation of bioconjugates. The characterization of AuNR bioconjugates was performed by independent measurements of AuNR and antibody concentrations. The change in antibody concentration in the presence of nanorods was estimated by a colorimetric protein assay.

Yang et al. (2008) reviewed the main progresses made over the past few years in the synthesis, surface modification, molecular assembly, and biological effects of gold nanorods. They explored their application prospects in photothermal therapy, biosensing, molecular imaging, and gene delivery. Later on, Abdelhalim et al. (2012) showed that the absorption intensity and maxima depends on the size of the nanoparticle. The red shift (from 517 to 532 nm) in SPR band was observed with increase in particle size of AuNP. These results clearly indicated that the fluorescence intensity and the absorption band of AuNP are size and concentration dependent.

Interactions of DNA with metals: Zhang et al. (2012) discussed the difficulties associated with attachment of DNA to silver nanoparticles at neutral pH by studying DNA adsorption kinetics. They attached the monothiolated DNA to silver nanoparticles at pH 3.0 in 30 minutes. Li et al. (2012) investigated the effect of monovalent cations (Li^+, Na^+, K^+, Cs^+) on self-assembly of thiol-modified double-stranded DNA (ds-DNA) and single-stranded DNA (ss-DNA) on gold electrodes. Electrochemical characteristics (surface coverage, ion penetration and charge transfer) of ds-DNA and ss-DNA self-assembled monolayers (SAMs) were formed with different monovalent cations and they have monitored the changes in their interactions.

Different methods of DNA & AuNP binding: The interactive studies on DNA-AuNP were started when Mirkin et al. (1996) for the first time shown the attachment between AuNP-DNA. Then different methods were introduced for making their attachment stronger. Experiments were performed with different types of DNA like single stranded and double stranded and different origin of DNA like calf thymus DNA and lambda virus DNA. Mirkin et al. (1998) developed protocols to assemble AuNP based on the site-selective hybridization of the molecular recognition properties of DNA. They had generated a method in which AuNP were first functionalized by oligonucleotides and then terminated with alkane thiol groups at the 3′ or 5′ positions.

Methods of improvement in binding of DNA with AuNP: Yang et al. (2003) studied the binding affinity of single stranded DNA (ssDNA) for gold nanoparticles surface. They indicated that the strength of interaction is dependent on particle size as small particles produced more pronounced effect.

Hurst et al. (2006) investigated the variables that influence DNA coverage on AuNP. The effects of salt concentration, spacer composition, nanoparticle size, and degree of sonication have been evaluated by them. By salt aging the nanoparticles to ~ 0.7 M NaCl in the presence of DNA containing a poly (ethylene glycol) (PEG) spacer, the loading was maximized. DNA loading was also increased by sonicating the nanoparticles during the surface loading process. Bacalocostantis et al. (2012) investigated that to what extend the binding of DNA to AuNP actually consists of only the sulfur bridge or if some other nonspecific binding mechanism was present. They reported high amount of strong, non-thiol mediated (nonspecific) binding of both single and double stranded DNA to AuNP.

Properties of DNA-Gold nanocomposites: Park et al. (2003) explained a simple model for the melting and optical properties of DNA-Gold nanoparticles aggregate. They also explained the physical details of gold nanoparticles in suspension when they show strong "surface plasmon" absorption in the visible range. Parado-Gotor et al. (2011) studied the interactions of the DNA molecule with NPs by non-covalent interactions, and more particularly with long DNA molecules.

Witten et al. (2008) was the first group who performed the systematic time-resolved *in situ* investigation of DNA-mediated AuNP assembly by UV/Vis-spectroscopy and dynamic light scattering (DLS). Characterization of the assembly at different temperatures showed a decrease of initial assembly growth rate with increasing temperature.

Major applications of DNA-Gold nanocomposites: Hutchison et al. (2003) have shown how a biopolymer, DNA, can be used as a scaffold for the assembly of extended, close packed, ligand-stabilized metal nanoparticle structures, including several desirable architectures (such as lines, ribbons, and branches). Electrostatic binding of ligand stabilized nanoparticles to the DNA backbone results in extended linear chain-like structures, ribbon-like structures composed of parallel nanoparticle chains, and branched structures.

Lin et al. (2009) demonstrated the bioconjugation of Au NP with DNA (DNA-Au NPs) for selective and sensitive detection of analytes such as mercury (II) ions, platelet-derived growth factor (PDGF), and adenosine triphosphate (ATP). They focused on approaches in which DNA-Au NP was used for colorimetric, fluorescent, and scattering detection of biopolymers. They highlighted the important roles that the size and concentration of Au NP and the length and sequence of DNA play in determining the specificity and sensitivity of the nanosensors for the analytes.

Eom et al. (2013) used the colorimetric property of AuNP to design the colorimetric sensing system for DNA-binding molecules using Non-Cross-Linking Aggregation. They developed the detection assay for determining the binding strength of DNA binding molecules to duplex DNA using a non-cross-linking mechanism. This allowed the discrimination between weak, intermediate, and strong intercalators using spectrometric instrument and the naked eye.

3. Rationale behind the present study

Currently, in many laboratories, research is going on using Au-DNA nanocomposites in the field of therapeutics, medications, gene therapies and biosensors. But optical properties and fluorescence intensity have not been much explored or even if used then there are very less amount of data available on these aspects. Fluorescence intensity values for sensing any biomolecule or metal ion using DNA-Gold nanocomposites have not been reported yet. Many biosensors are present but they are based on different sensing mechanisms. Influence of size and shape of AuNP on its optical properties have been studied but there have been very less data generated on change in DNA conformation due to change in the size and shape of nanoparticles. Moreover, very less in known about the effect on optical activity of AuNP in the presence of double stranded DNA.

Keeping in view with the above, Scheme 1 is proposed below to outline the rationale of the present study. This refers to diagrammatical representation of AuNS binding with DNA to form DNA-Gold nanocomposites. Subsequently, these nanocomposites need to be treated with different metal ions such as magnesium (Mg^{2+}), calcium (Ca^{2+}) and iron (Fe^{2+}) ions. The effects of these ions on DNA-Gold nanocomposites are to be studied carefully and categorically. The effects of these ions could be studied by change in fluorescence intensity, which will help in determining the concentration of Mg^{2+} ions in any solution.

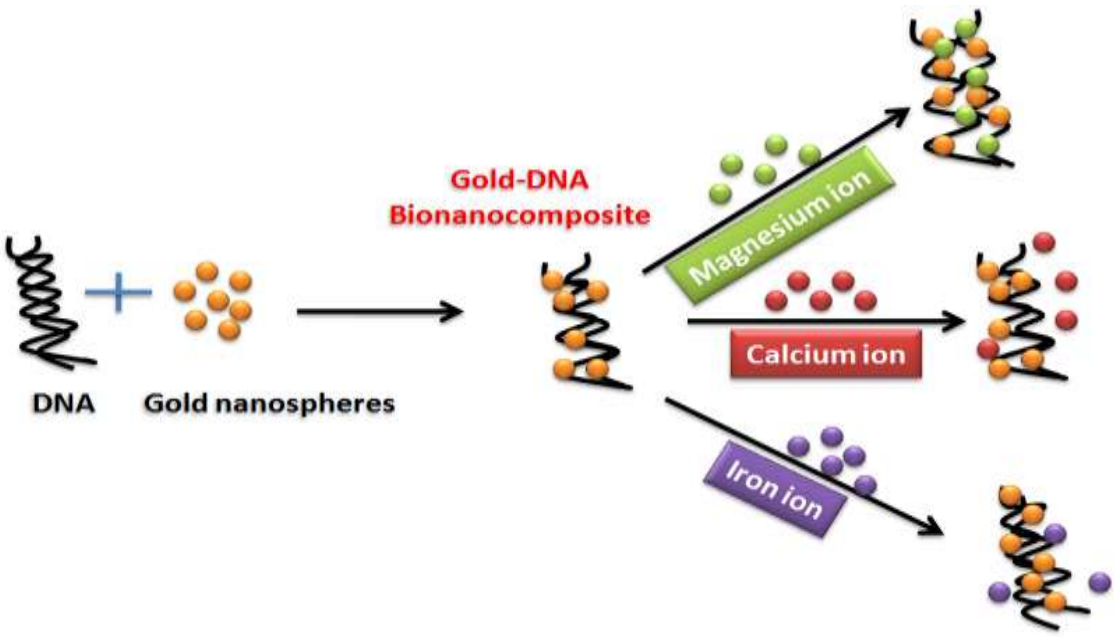

Scheme 1 Diagramatic representation of the present study

4. Objectives

- To study the variation in the optical phenomenon on binding of AuNP with DNA
- To study DNA-Gold Nanocomposites' optical, structural and electro kinetic properties
- To study the effect on optical properties by changing size and shape of the nanoparticles
- To study their efficacy as biosensor

5. Materials and Methods

5.1. Materials

Chemicals: Chloroauric acid ($HAuCl_4$) was purchased from Loba Chemie. Cetyltrimethylammonium bromide (CTAB) and DL-Dithiothreitol solution (DTT) were purchased from Sigma Aldrich. Ice cold Sodium borohydride ($NaBH_4$) was purchased from Rankem and Silver Nitrate ($AgNO_3$) was purchased from Fisher Scientific. Ascorbic acid and Meta propionic acid (MPA) were purchased from Loba Chemie. Deionized water was obtained using an ultrafilteration system (Milli-Q, Millipore) with a measured conductivity above 35 mho cm^{-1} at 25˚C.

DNA materials: DNA from two different origins was used. One was lambda DNA and another was Herring sperm DNA, purchased from Sigma Aldrich and Merck Biosciences, respectively.

5.2. Synthesis of Gold nanospheres of different sizes

Gold nanospheres (AuNS) were prepared by seed mediated method (Panikkanvalappil R. Sajanlal et al. 2010). The seed solution was prepared by adding 250 μL of 10 mM $HAuCl_4$ to 10 mL of 100 mM Cetyltrimethylammonium bromide (CTAB) with brief, gentle mixing. Next, 600 μL of freshly prepared, ice-cold 10 mM $NaBH_4$ solution was added followed by mixing for 2 min. The pale brown seed solution was prepared which was stable and usable for several days.

The AuNS growth solution was prepared by adding the following order and then gently mixing: 40 mL of 100 mM CTAB, 1.7 mL of 10 mM $HAuCl_4$.$3H_2O$and 250 μL of 10 mM AgNO3. Next, 270 μL of 100 mM ascorbic acid was added, which changed the solution from brown-yellow to colorless. To initiate nanospheres growth 460 μL of the seed solution was added to the growth solution, mixed gently and left still for 1h. These AuNS served as medium and changed to different sizes on increasing the refluxing time from 2-4 h. From these AuNS, additional CTAB was removed by centrifugation and washed with water for five times and finally dispersed in 3 mL de-ionized water.

5.3. Synthesis of Gold nanorods

Au nanorods (NR) were synthesized by the addition of 220 μL of above prepared seed solution into the aqueous mixture (40 mL) containing CTAB (100 mM), $HAuCl_4.3H_2O$ (1.7 mL, 10 mM), $AgNO_3$ (250 μL, 10 mM) and ascorbic acid (270 μL, 100 mM). The appearance of deep blue color solution showing transverse surface plasmon (TSP) band at

539 nm and longitudinal surface plasmon (LSP) band at 697 nm indicated the formation of AuNR (Edgar et al. 2012). The as-synthesized AuNP were washed with de-ionized water under centrifugation at 8500 rpm for 10 min (P´erez-Juste et al. 2005).

5.4. Preparation of DNA-Au nanocomposites

Firstly, UV light of laminar hood was ON for 15 min before use. At the time of use, UV light was switched off and laminar hood surface is swapped with acetone to make it sterilize. 20μL of DNA (3.5 mg/mL) was diluted with 2 mL of autoclaved water (Zhang et al. 2012). 5 μL of mercaptopropanoic acid (MPA) was added and incubated at 21°C for 24 h to ensure the binding of alkane thiol to oligonucleotides (Witten et al. 2007). Before use, the disulfide bonds formed by the oligonucleotides due to mercaptopropanoic acid was cleaved by adding DTT to the above solution and incubated at room temperature for 1h (0.1 M DTT, 10 mM phosphate buffer). To remove all unbound alkane thiol-double stranded DNA from solution, the DNA functionalized gold nanoparticles were washed two times by centrifugation (13000 rpm, 15 min) and re-dispersed in fresh autoclaved water.

5.5. Characterization of DNA-Au nanocomposites

Various techniques are used to characterize gold nanoparticles and DNA functionalized gold Nanocomposites. The technical details of these techniques are given below:

Ultraviolet-Visible (UV-Vis) Spectrophotometeric analysis: The optical property of AuNS and AuNR was analyzed by UV-Vis (Specord 205) spectrophotometer. 1 mL of each and every synthesized AuNS and AuNR was diluted by 2 mL of de-ionized water. Then there UV–Vis absorption spectra were obtained. It is followed by adding 1ml of Au-NS and Au-NR into 2 mL of DNA sample (4.5 ng / μL). The shift in surface plasmon bands were also depicted by this instrument.

Circular Dichorism (CD) Spectrophotometeric analysis: Electronic CD spectra were recorded in a BioLogic Mos-450 spectropolarimeter. A standard quartz cell of 10 mm path length was used. The spectra were expressed in terms of molar ellipticity. Scans were taken from 200 nm to 900 nm for the intrinsic region. For each spectrum 5–10 runs were averaged at a constant temperature of 298.2 K. Reversible conformational change of DNA was studied after binding with AuNS and AuNR, respectively.

Zeta potential & Dynamic Light scattering (DLS) analysis: Zeta potential is used to study the electro-kinetic parameter of the sample. The properties i.e. DLS, zeta potential, conductance

and mobility of different AuNS and AuNR were analyzed in 2 mL of solution using Brook heaven 7610.

Transmission Electron Microscopy (TEM) analysis: For TEM examinations, a single drop (10 μL) of the aqueous solution of the gold nanoparticles was placed on a 300 mesh copper grid coated with a carbon film. The grid was left to dry in air for several hours at room temperature. TEM analysis was carried out in a Hitachi S-500 electron microscope working at 30 kV.

FTIR Spectrophotometeric analysis: The change in bonds after adding AuNS and AuNR in DNA solution was analyzed by. It is a way to check the confirmation of DNA-Gold nanoparticle binding.

Atomic Force Microscopy (AFM) analysis: AFM images were obtained with a Multimode AFM (with Nanoscope V controller). A standard silicon cantilever from Nanosensors with a resonance frequency around 45–115 kHz was used for performing the tapping mode. Sample for AFM analysis was prepared by placing 50 μL nanoparticle solutions on a silicon wafer and was allowed for complete evaporation before imaging. Image processing was carried out with Nanoscope software from Burker, Germany.

Fluorescence Spectrophotometeric analysis: Fluorescence measurements were analyzed by Perkin-Elmer LS55, interfaced to a PC for the reading and handling of the spectra. DNA-AuNP interaction with different metal ions was also studied through this instrument. The excitation and the emission wavelengths were 260 nm and 250 nm respectively.

6. Results & Discussion

6.1. Agarose Gel Electrophoresis of DNA

The quality of the DNA samples was checked through agarose gel electrophoresis. The DNA samples, Herring sperm and λ DNA were run on 0.8% Agarose gel in 0.5X TBE buffer as shown in Figure 3. λ DNA is a genomic DNA and a bright thick smear appeared on the gel. In the Herring sperm DNA, light smear was observed indicating the presence of DNA in the form of oligonucleotides (Li et al., 2013).

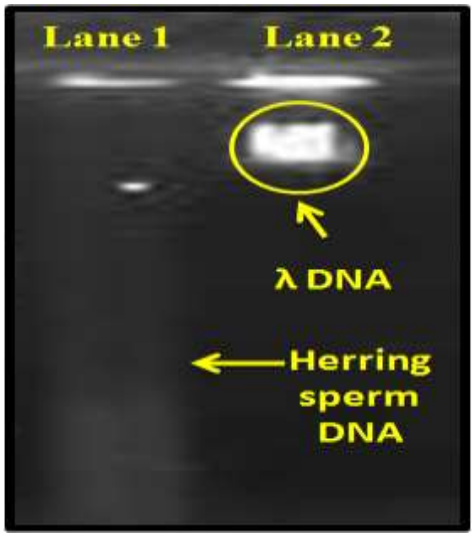

Figure 3. Agarose gel electrophoresis of DNA. Lane 1 Herring sperm DNA; Lane 2 Bacteriophage λ DNA

6.2. Optical Analyses

Optical analysis can be defined as the study of properties of a substances or sample, such as its chemical composition or the size of particles present in it, through observation of effects on transmitted light, such as scattering, absorption, refraction and polarization. It can be studied by various instruments like UV-Visible spectrophotometer, CD spectrometer and polarimeter. In UV-Vis spectrophotometer and CD spectrometer, optical analysis is conducted by observing the change in absorbance. Polarimeter gives the value of optical rotations. Here results of UV-Vis spectra and CD spectra are discussed.

6.2.1. UV-Visible spectra of Au nanoparticles

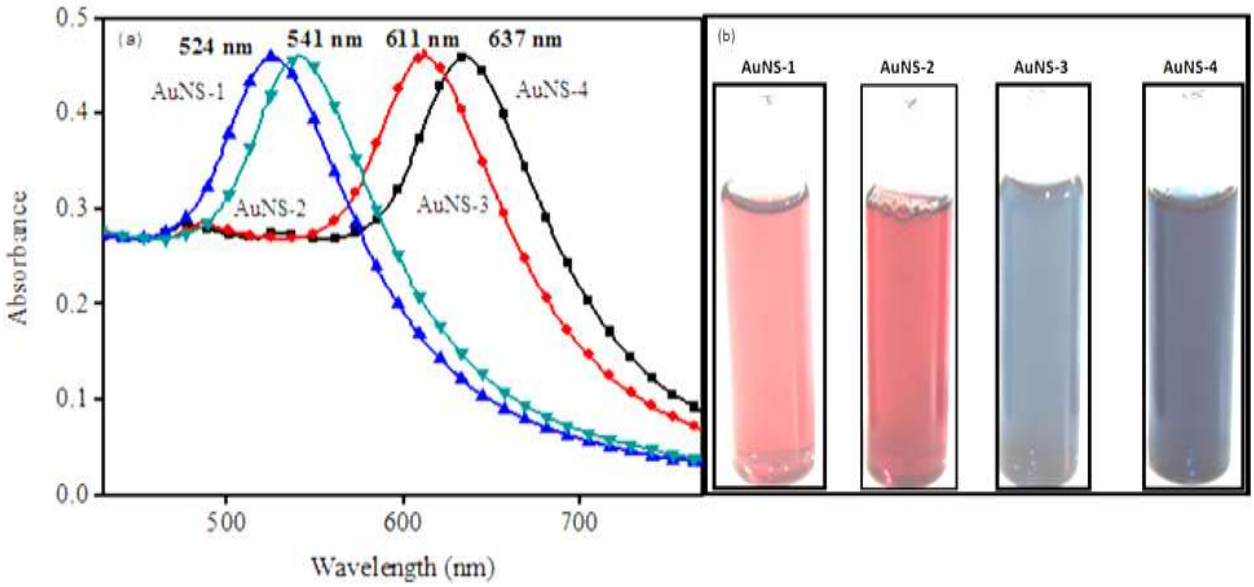

Figure 4. (a) UV-Vis spectra and (b) colour of different sizes of AuNS

Figure 4(a) shows the surface plasmon resonance (SPR) bands of four different sizes of AuNS (Kim et al. 2008) and the corresponding figure 4(b) represents their various colors (Lin et al. 2009 & Lim et al. 2012). A single SPR band ranging from 524-637 nm has been observed as a function of their size (Khlebtsov et al. 2010). The red shift in SPR band from 524 nm to 637 nm indicates the increase in size (Liao et al. 2005). Figure 5 represents two SPR bands, namely transverse (539 nm) and longitudinal (697 nm) for the AuNR (P´erez-Juste et al. 2005). According to Mie's theory, single SPR band is observed for the nanospheres and for anisotropic particles, more than one SPR bands are observed.

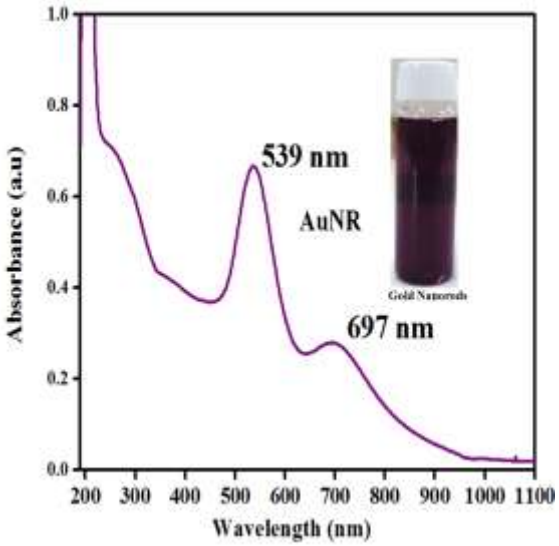

Figure 5. UV-Vis spectra of Gold nanorods

6.2.2. UV-Visible spectra of DNA-Au nanocomposites

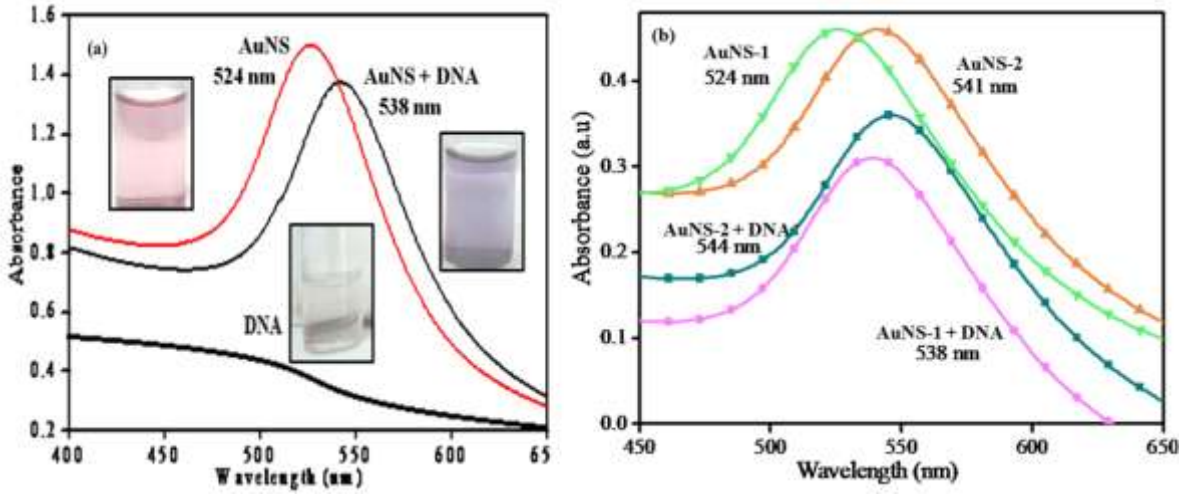

Figure 6. Shift in UV-Vis spectra of (a) AuNS with change in colour and (b) AuNS-1 and AuNS-2 on addition of DNA.

The binding of DNA with AuNS and AuNR resulted in the red shifts of SPR bands from their respective positions (Storhoff et al. 1998). In figure 6(a) the SPR UV-Vis spectra of AuNS corresponding to 524 nm, shifts to 538 nm on addition of DNA, while DNA doesn't show any band in this region. Same shift was observed in AuNS-2 in figure 6(b).This shift occurred, probably due to close contact of dispersed gold nanoparticles resulted on the addition of DNA (Yang et al. 2003). Similar results were obtained for different sizes of

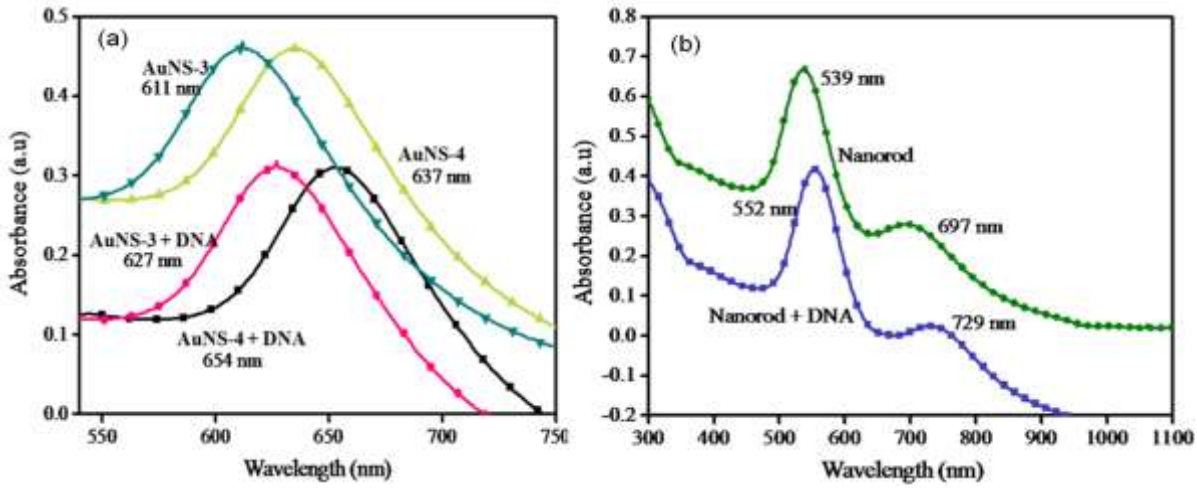

Figure 7. Shift in UV-Vis spectra of (a) AuNS-3 and AuNS-4 (b) Gold nanorods (AuNR) on addition of DNA

AuNS and AuNR as shown in figure 7 (a) and (b), (Brown et al. 1998; Storhoff et al. 1999 & Wang et al. 2012). It might be due to the aggregation of gold nanoparticles on binding with DNA.

The results shown in figures 6 and 7 are summarized in table 1. For AuNS, there is a shift of 15 nm in λmax, on an average. Values of λmax shown in the Table 1 clearly indicate the change in SPR band on binding of DNA with AuNS. Maximum shift was observed with AuNS-4 as its λmax corresponding to 637 nm shifted to 654 nm. AuNS-4 is larger in size as compare to other AuNS.

Table 1. Showing shift in λmax on adding DNA to gold nanospheres:

S.No.	Sample	λmax before addition of DNA (nm)	λmax after addition of DNA (nm)	Shift in wavelength (nm)
1.	AuNS-1	524	538	14
2.	AuNS-2	541	544	3
3.	AuNS-3	611	627	15
4.	AuNS- 4	637	654	17

In case of AuNR, maximum λmax was observed in its longitudinal peak as compared to its transversal peak. The shift in λmax is of 13 nm and 28 nm for transversal and longitudinal peaks, respectively. The loading of DNA might be maximum at longitudinal cross-section of AuNR, therefore major shift was observed in this region.

6.2.3. CD spectra analysis

Circular Dichroism (CD) refers to the differential absorption of left and right circularly polarized light. It is exhibited by biological molecules, because of their dextrorotatory and levorotatory components. In DNA, formation of helical structure is a super asymmetry that gives rise to degenerate interactions between chromophoric bases and results in intense CD spectra. DNA functionalized gold nanoparticles binding causes a conformational change in the DNA structure which can be observed by this technique. The backbone conformation of DNA showed a characteristic of right-handed B form in the far UV region (220-320 nm). The CD spectrum of free DNA has a negative peak at 247 nm and a positive peak at approximately 278 nm which corresponds to B-DNA. These bands were formed due to stacking interaction between the bases and the helical structure of DNA which provided asymmetric environment for the bases (Goodman et al. 2006).

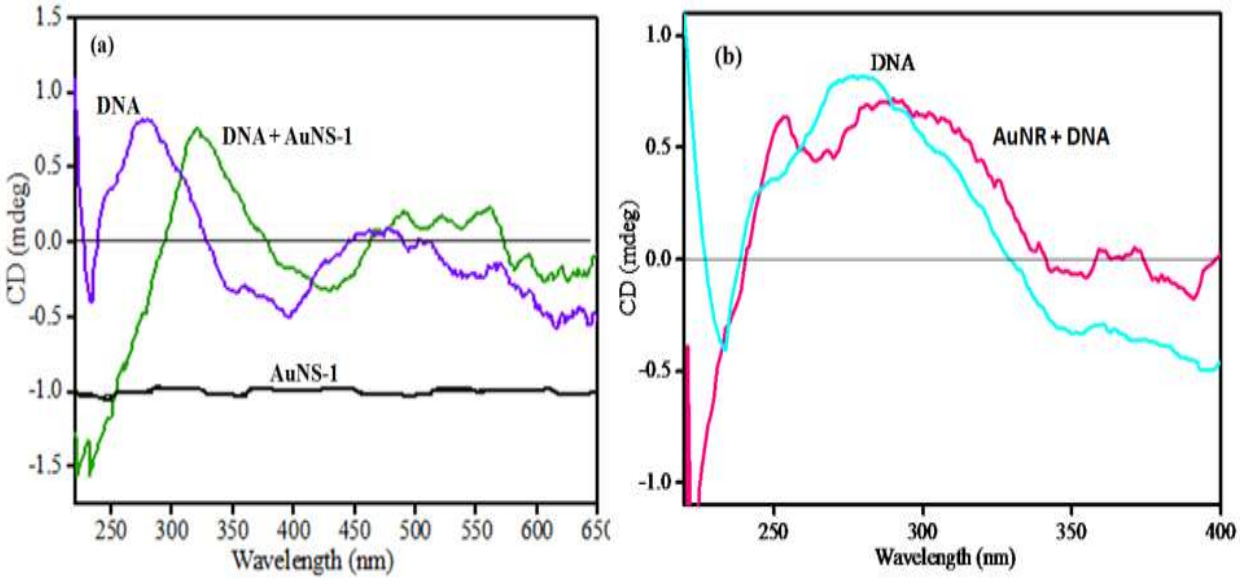

Figure 8. Change in DNA's conformation on binding with (a) AuNS-1 and (b) AuNR

As shown in figure 8(a), upon the addition of AuNS-1 to DNA solution, the molar ellipticity decreased at approximately 220 nm and increased by approx. 280 nm (Sandström et al. 2003). These changes coupled with a shift in the maximum wavelength of the positive band indicate partial denaturation (Prado-Gotor et al. 2011). Same changes were observed in figure 8(b), when AuNR was added to DNA solution. These changes indicate the conformational change in DNA on binding with AuNP.

6.3 Size and Shape Analysis

Size and shape analysis of nanoparticles present in a solution, is of great importance. The size and shape can affect the appearance and stability of the solution. There are various techniques through which analysis can be done like TEM, SEM and DLS. TEM and SEM are used for structural and morphological analysis of nanoparticles. DLS is used to determine the size distribution profile of nanoparticles present in a given solution. The TEM and DLS results are used in this study to measure the size of AuNS and AuNR.

6.3.1. Transmission Electron Microscopy (TEM)

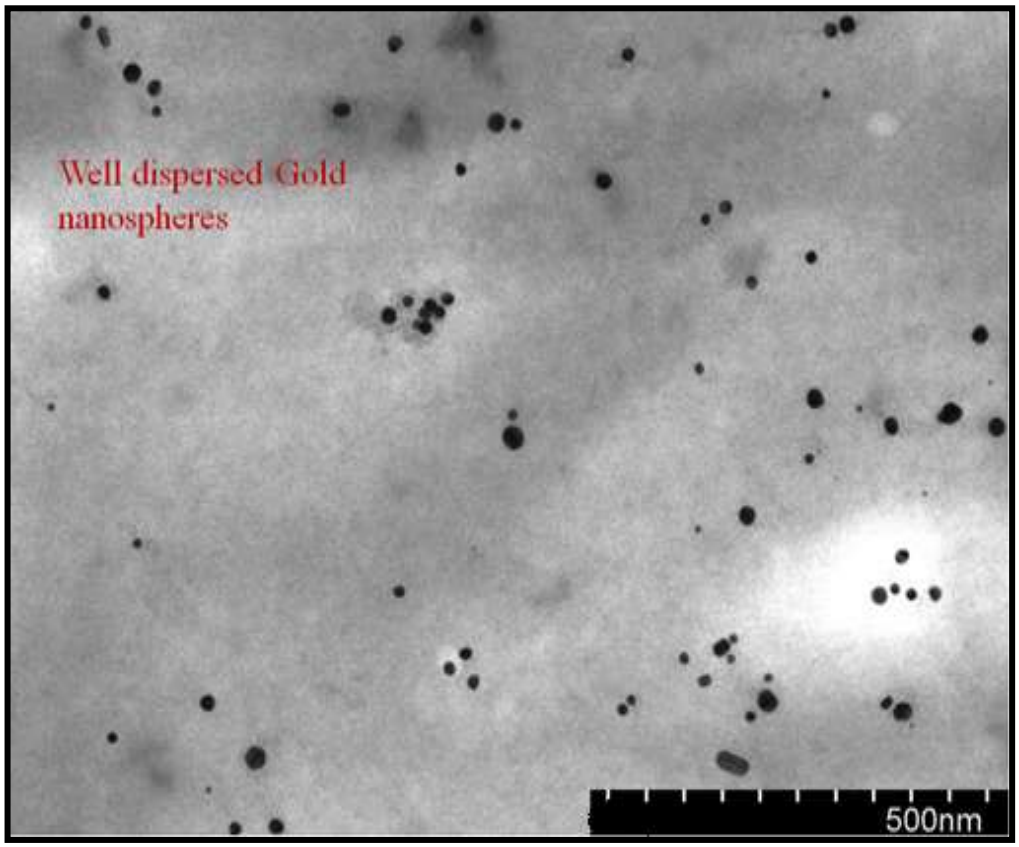

Figure 9. TEM image of Gold nanospheres

Transmission electron microscopy (TEM) is a sophisticated technique through which size and position of particle can be determined. The TEM image shown in Figure 9 reveals the formation of almost spherical Gold nanospheres of around 33-36 nm size (Ganguly et al. 2013). These gold nanospheres were found to be lying separate from each other due to the coating of CTAB on their surface because it lends them a positive charge (Kim et al. 2008).

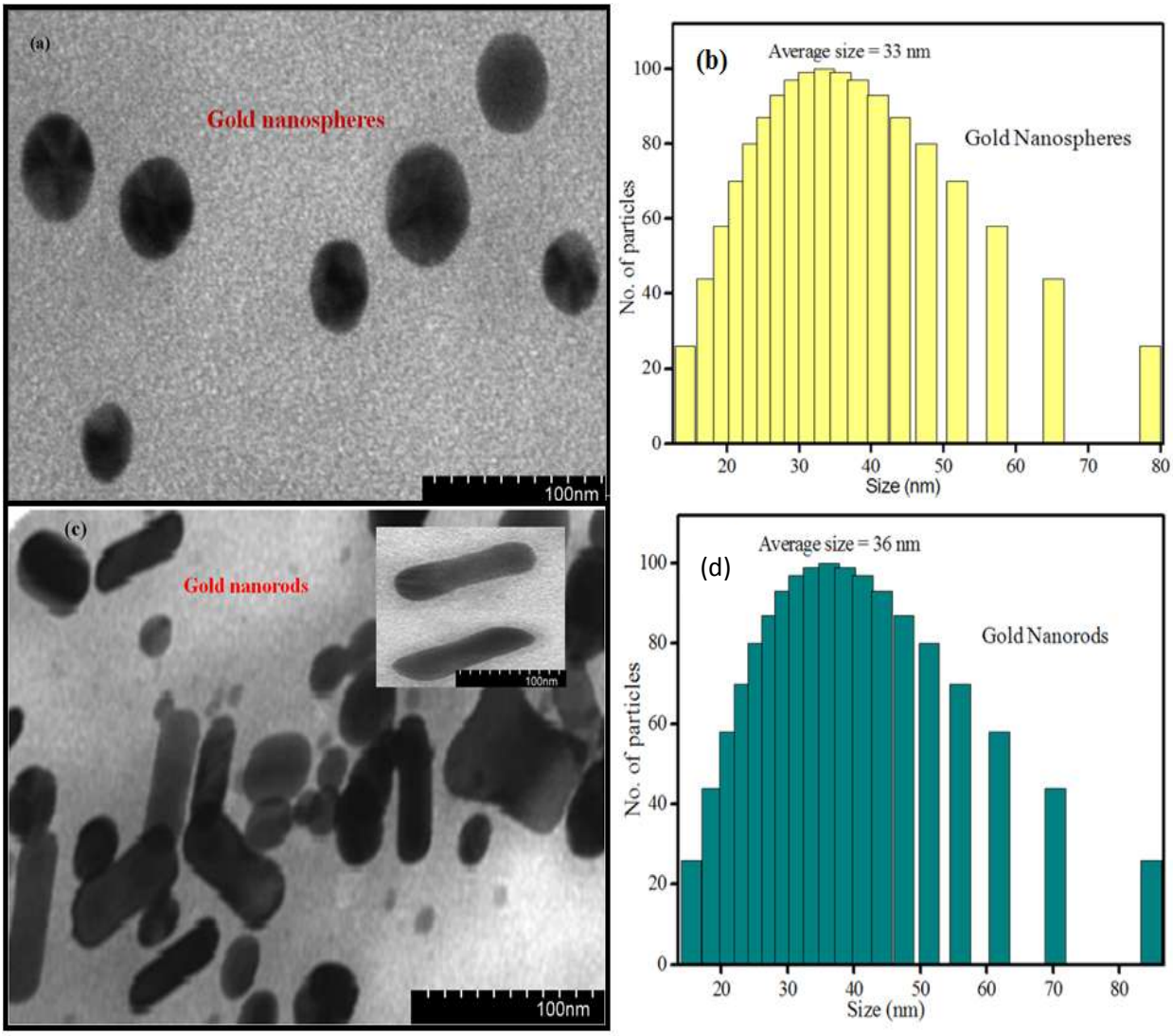

Figure 10. TEM Image with DLS of Gold nanospheres (a) and (b) and Gold nanorods (c) and (d)

In figure 10 the TEM images of AuNP is shown along with their DLS (Tsai et al. 2008). From figure 10(a), size of AuNS calculated was approximately 40 nm which was equivalent to the average size i.e. 33 nm determined by DLS in figure 10(b) (Nakao et al. 2003). Image of AuNR is shown in figure 10(c) (Liao et al. 2005 & Wang et al. 2012). The size determined by DLS graph for AuNR was 36 nm. Along with AuNR many other AuNP of different size and shapes were also present in the sample.

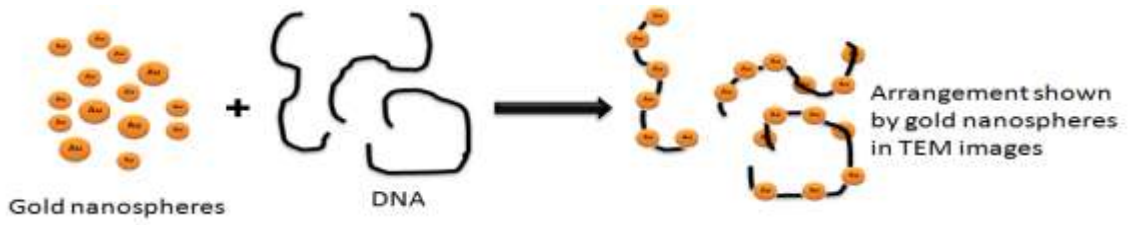

Scheme 2 Pictorial representation of patterns of AuNS after binding with DNA

The scheme 2 shows the pattern of AuNS on binding with DNA which is a representation of TEM images [Figure 11(a)] (Warner et al. 2000).

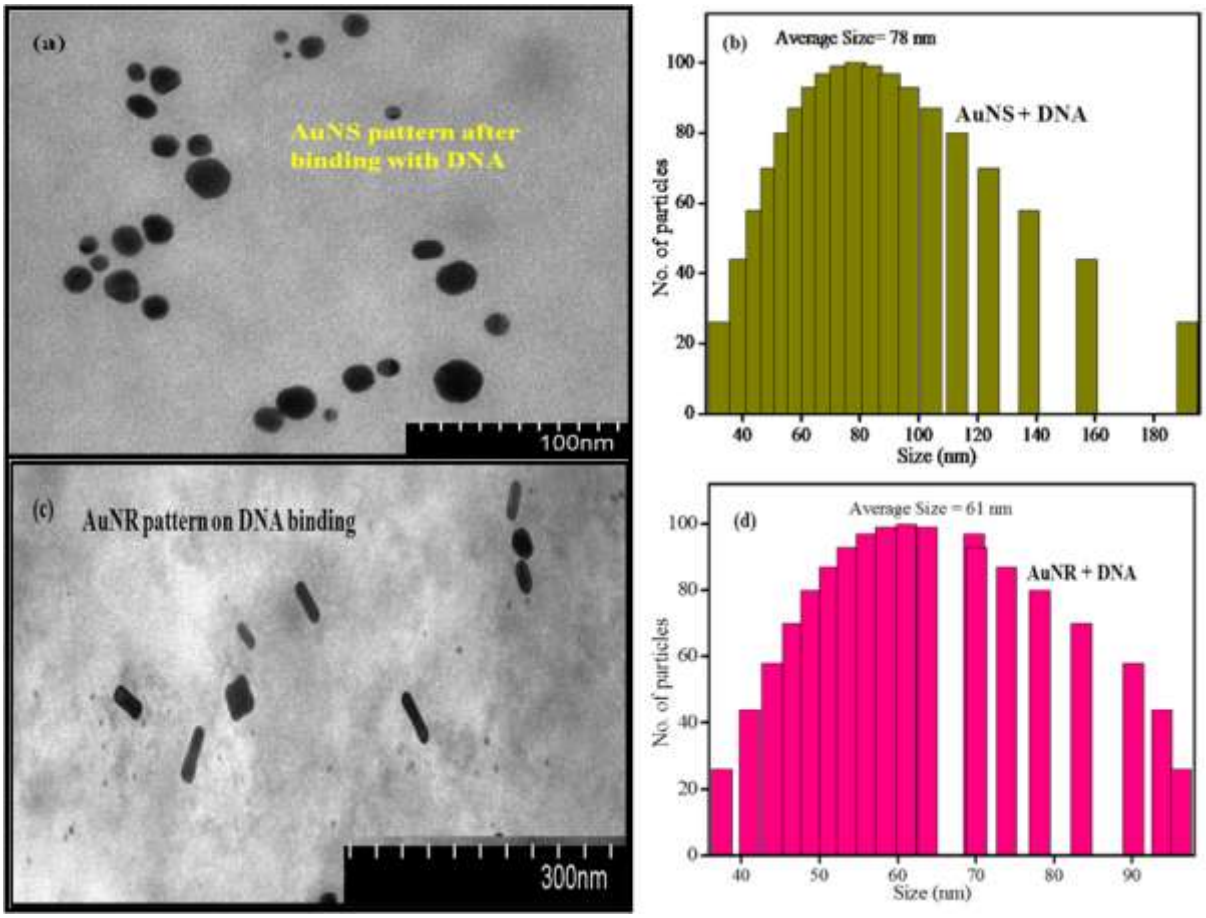

Figure 11. TEM image showing pattern of (a) AuNS and (c) AuNR with their DLS (b) and (d) respectively, after addition of DNA

Through the TEM images shown in figure 11, it was concluded that on binding of AuNP with DNA, a particular pattern was followed and there was a complex formation of DNA with AuNS and AuNR [figure 11(b) & 11(d)] determined by DLS (Yang et al. 2003). The complex formed was considered as DNA-AuNP nanocomposites. It is the technique which helps in determining the size of the particle present in the given sample (Liu et al. 2007 & Li et al. 2010). As DNA is a polynucleotide and it ranges from 2 nm to 2000 nm, the instrument used for DLS cannot determine the particle size below 4 nm and above 200 nm. This is the reason for unavailability of DNA size through DLS. As shown in figure 10 (b) & 10 (d), AuNS and AuNR were 33.42 nm and 47 nm in size, respectively. After binding of DNA to the AuNP, the change in size was observed. As the size of AuNS changed from 33 nm to 78 nm, it confirmed the binding of DNA to AuNS and AuNR.

6.3.2 Atomic Force Microscopy (AFM)

AFM images were obtained which confirmed the binding of functionalized DNA with AuNP. Although the images were not very clear but as per the data obtained from literature, it shows the changes in positions of the AuNS and AuNR (Hegner et al. 1993). From figure 12(a) & (b) we can see the even distribution of gold nanoparticles in the solution.

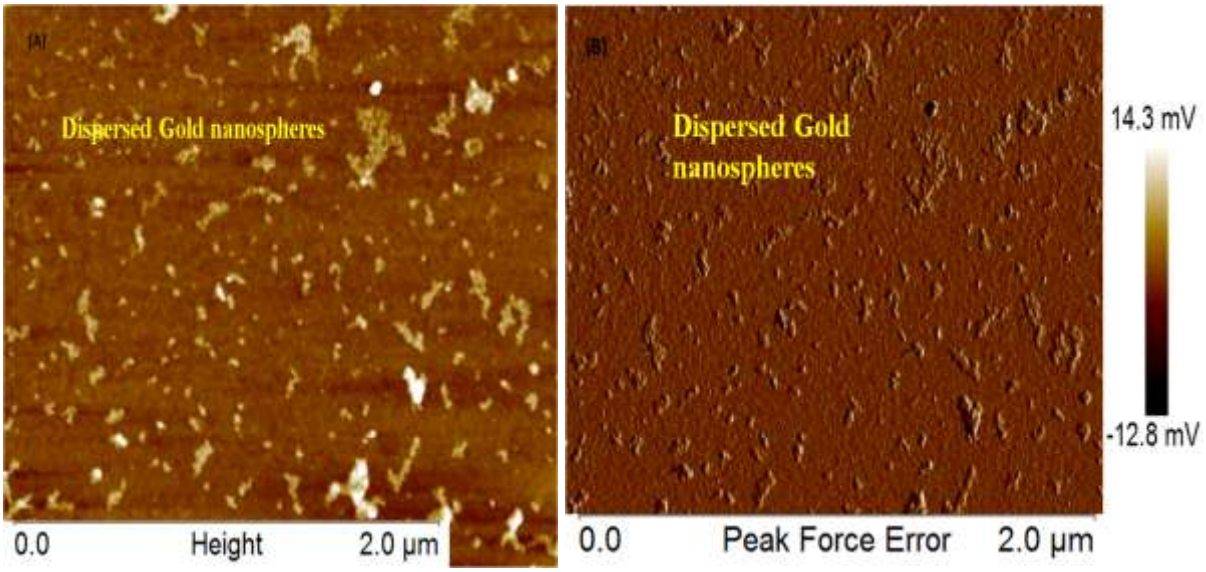

Figure 12. Image of Gold nanospheres in (a) Height mode and (b) Amplitude mode

The AFM image of figure 12(a) shows the distribution of Gold nanospheres on the silicon wafer which indicates the proper dispersion of gold nanospheres in the solution (Nakao et al. 2003). The height range was taken from 0-2 µm. Peak error in the image of gold nanoparticles is shown in figure 12(b) (Storhoff et al. 1999 & Li et al. 2013). The amount of current passed at the time of movement of tip of cantilever over the surface was also monitored in amplitude form and its range was between -12.8 mV to 14.3 mV (Brown et al. 1998).

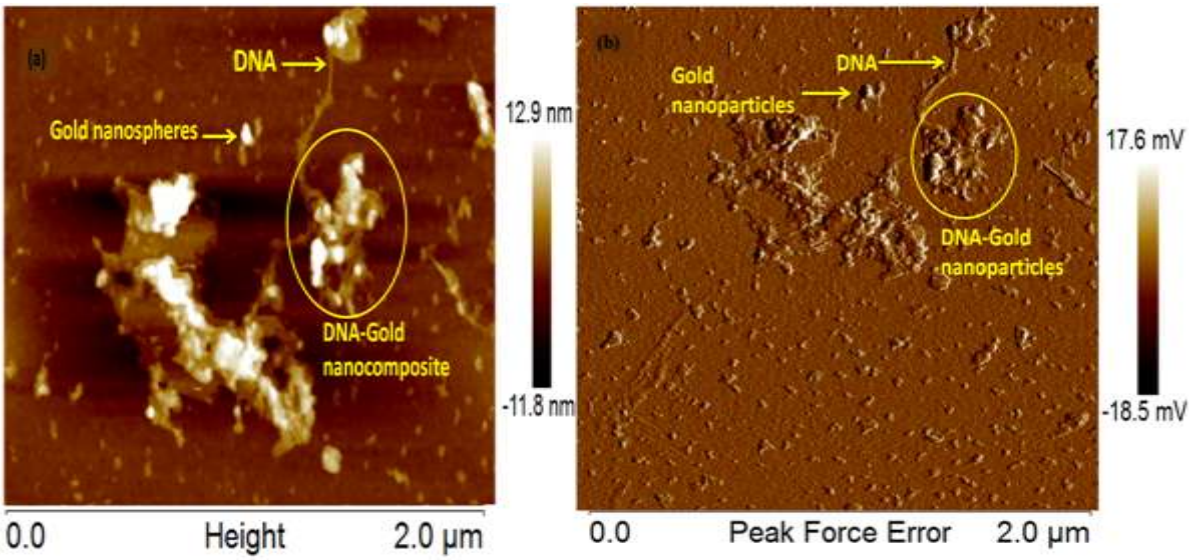

Figure 13. Images of DNA-Gold nanocomposites showing (a) Height Mode and (b) Amplitude mode

The images shown in the figure 13 have confirmed the presence of DNA. In the solution, DNA was clearly seen as thread like structure in figure 13(a). The complex of DNA-AuNS was also observed and it led to the structural confirmation of binding of functionalized DNA with AuNP. The amplitude range obtained for DNA-Gold nanocomplex amplitude was higher than the amplitude range of only AuNS.

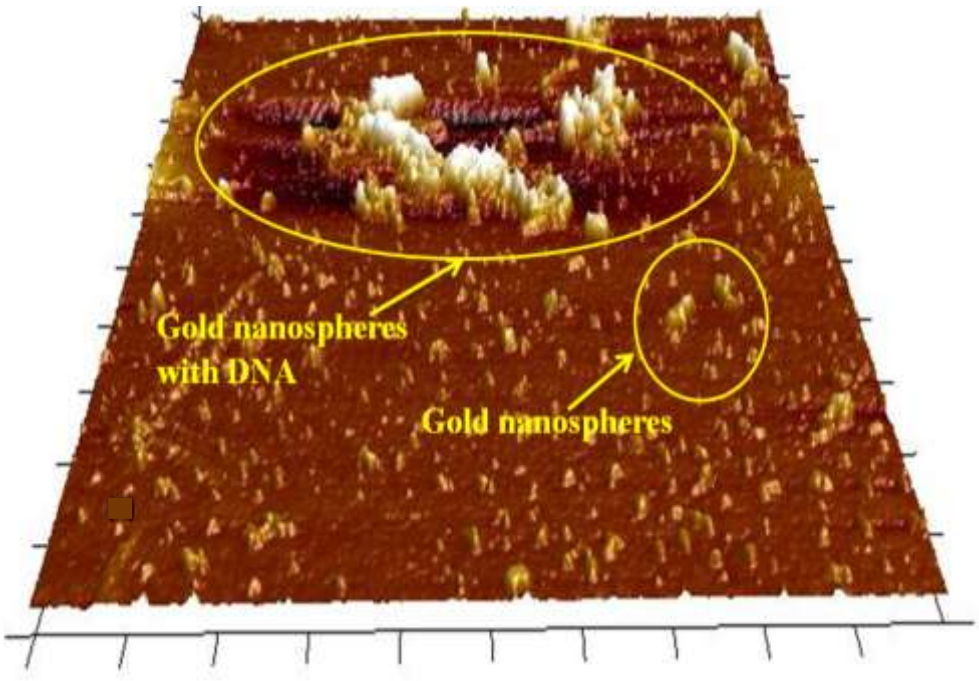

Figure 14. AFM 3-D image of DNA-Gold nanocomposite

The 3-D height mode image shown in figure 14 is a different format of AFM image in which three dimensional image of the sample is shown. In the image, whole silicon wafer is shown on which DNA-Gold nanospheres sample was placed and allowed for complete evaporation before imaging. Here gold nanospheres are shown to be well dispersed but at the upper part on the slide, the clusters appeared and those were considered as DNA-Gold nanocomposites.
DNA web appeared as shown in figure 15. It might be due to clustering of gold nanorods

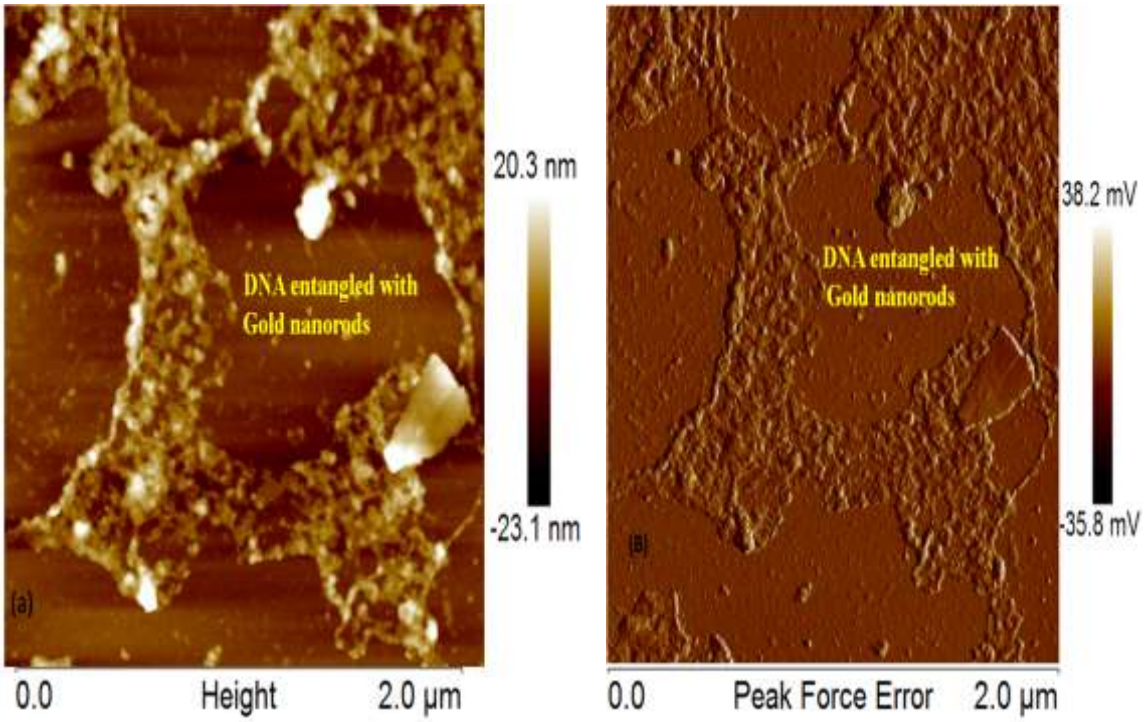

Figure 15. Images of DNA-Gold nanorods complex in (a) Height mode and (b) Amplitude mode

around the DNA. As shown in figure 15(a), the height of the sample from the surface was estimated to be around 20.3 nm. The brighter areas on the image had the maximum height of 20.3 nm. Figure 15 (b) shows the amplitude of DNA-AuNR i.e. 38.2 mV.
The size of nanoparticles shown in this image was smaller than the size of nanorods shown in image. Here the nanorods were of 19.8 nm size. DNA in the form of small polynucleotides is also shown in the image (Liao et al. 2005)

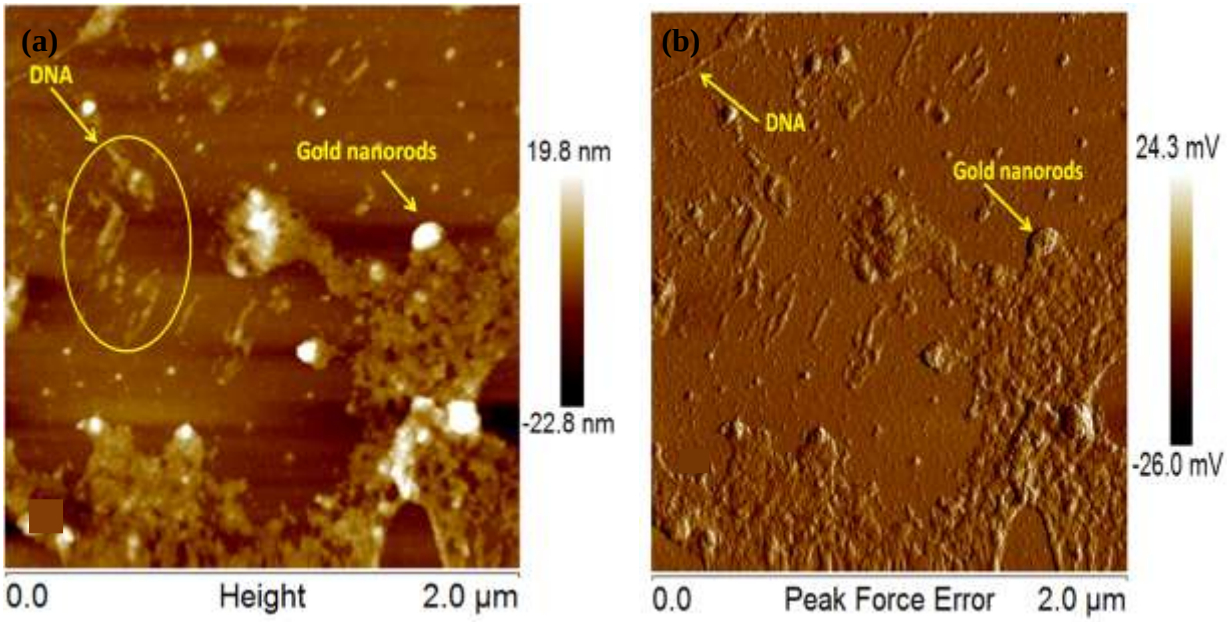

Figure 16. AFM images of DNA and AuNR in (a) Height mode & (b) Amplitude mode

From the figure 16 (a) and (b), the amplitude was measured to be 23.4 mV for nanorods of size 19.8 nm. It is known that smaller the size of particle more will be the value of amplitude. The amplitude determines the distance of particle from the tip of cantilever.

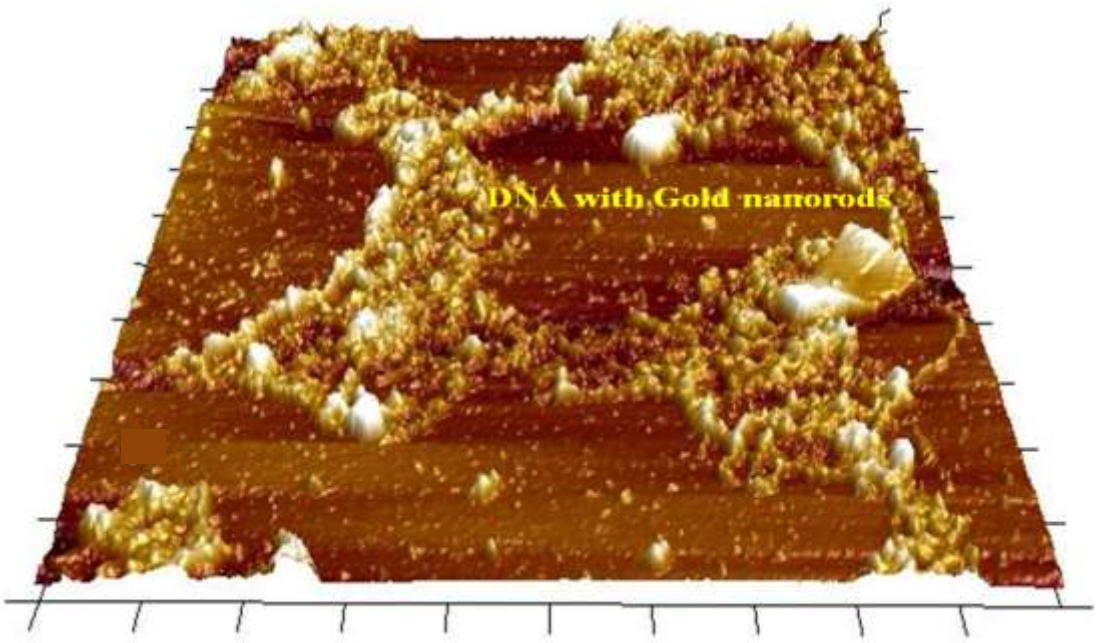

Figure 17. 3-D image of DNA with gold nanorods

In Figure 17, the clustering of DNA and AuNR has been shown in 3-D form. AuNR distribution on the silicon coated slide has been seen in this image.

6.4 Electrokinetic analysis

Electrokinetic analysis includes zeta potential, conductance and charge.

6.4.1 Zeta potential

Zeta potential can help in determining the charge and stability of the particles present in the sample. DNA sample have negative charge due to the presence of phosphate group at their backbone (Bacalocostantis et al. 2012). Negative charge of DNA slightly decreased on binding of mercaptopropanoic acid (MPA). The gold nanospheres synthesized had CTAB coating which is positive in nature.

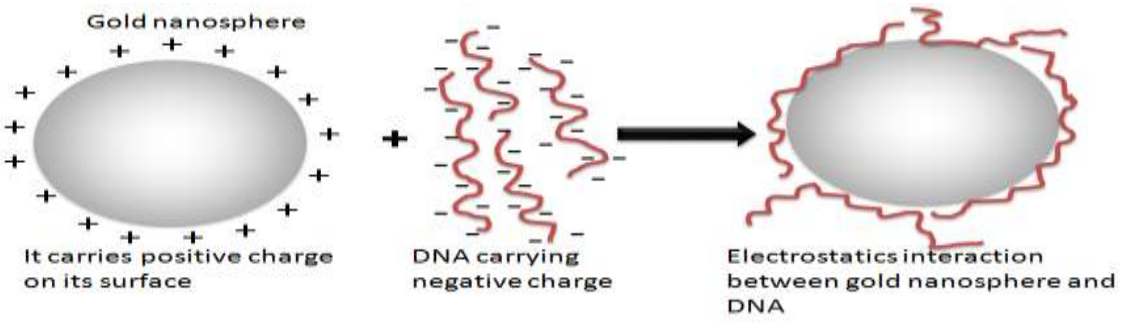

Scheme 2 Pictorial representation of electrostatics interaction between DNA and AuNP

The scheme 2 shows the formation of DNA-Gold nanocomposite due to electrostatic interaction between them. The values obtained for zeta potential, conductance and mobility are summarized in table 2.

Table 2. Variation in zeta potential, conductance and mobility of AuNP on addition of DNA

S.No	Sample Name	Zeta Potential	Conductance	Mobility
1.	DNA	-16.84 mV	183 µS	- 1.28
2.	DNA + MPA	-7 mV	20 µS	1.78
3.	AuNS	+ 22.8 mV	277 µS	1.30
4.	AuNS + DNA	+16.67 mV	270 µS	- 6.17
5.	AuNR	+26.16 mV	348 µS	2.04
6.	AuNR + DNA	+10.40 mV	305 µS	0.81

In table 2, it has been shown that zeta potential of DNA i.e. -16.84 mV on binding with AuNS and AuNR changed to +16.67 mV and +10.40 mV, respectively. The zeta potential of AuNS and AuNR before binding with DNA was +22.8 mV and +26.16 mV, respectively. Along with changes in zeta potential, change in mobility and conductance was also observed. This gives an idea about electrostatic interaction between DNA and AuNP.

7. Metal ion detection

In recent years, nanoparticles have received much attention in the field of biosensing due to their exquisite sensitivity in chemical and biological sensing (Ganguly et al., 2013). Among the nanoparticles used as biosensors, AuNP has gained more interests because of its several intriguing properties. One of its properties which is used for detection is the fluorescence when gold nanoparticles combine with DNA (Li et al. 2013). In the figure 18, it is clearly shown that at excitation of 260 nm, the AuNS has not exhibited any fluorescence but bare Herring sperm DNA used for detection has shown fluorescence. The solution having complex of DNA with AuNS has shown higher fluorescence intensity than bare DNA (Bacalocostantis et al. 2012).

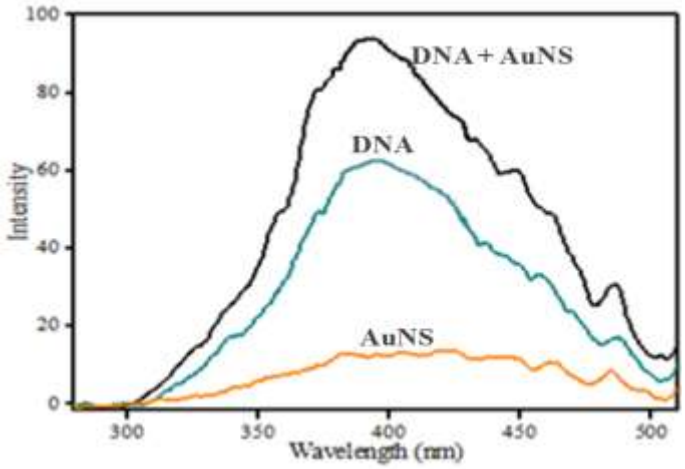

Figure 18. Graph showing increase in fluorescence intensity of DNA on binding with gold nanospheres

It might be due to the opening of double stranded DNA because of binding of AuNP, which leads to the increase in fluorescence.

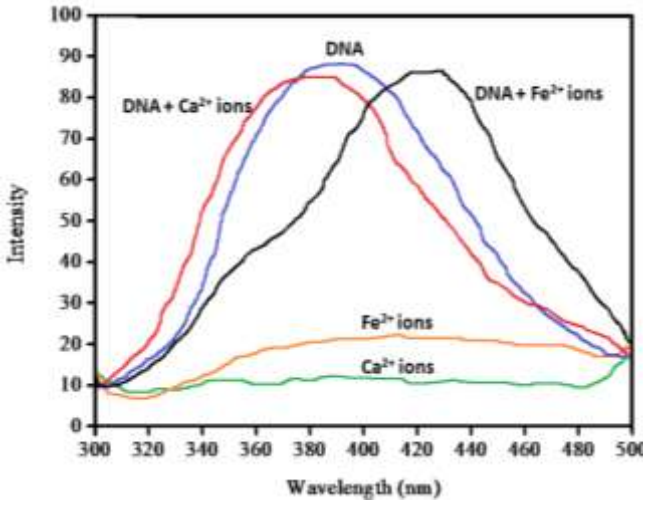

Figure 19. Fluorescence spectra of Fe^{2+} and Ca^{2+} metal ions

DNA-Gold nanocomposites were used as a system to detect the presence of metal ions in any solution. Three metals Calcium (Ca), Iron (Fe) and Magnesium (Mg) were chosen as detection target because these metals are highly abundant in nature. There are various sophisticated electrochemical techniques available which are used to detect these metals. But these techniques are highly complicated and required expertise in handling. Instead DNA-Gold nanocomposites as a metal detector are very convenient to use and time effective.

From the graph shown in figure 19, it can be observed that calcium ion has not produced any fluorescence and even on adding calcium ions in Herring sperm DNA solution there was no change in the fluorescence of DNA. The intensity of bare DNA and calcium ion added DNA was same. It is evident from the graph that calcium ions were not affecting the fluorescence intensity. Similarly, iron ions were also not affecting much fluorescence intensity (Guha et al. 2011). But on addition of Mg^{2+} ions in the DNA solution, there was an increase in the intensity of DNA (Fan et al., 2011).

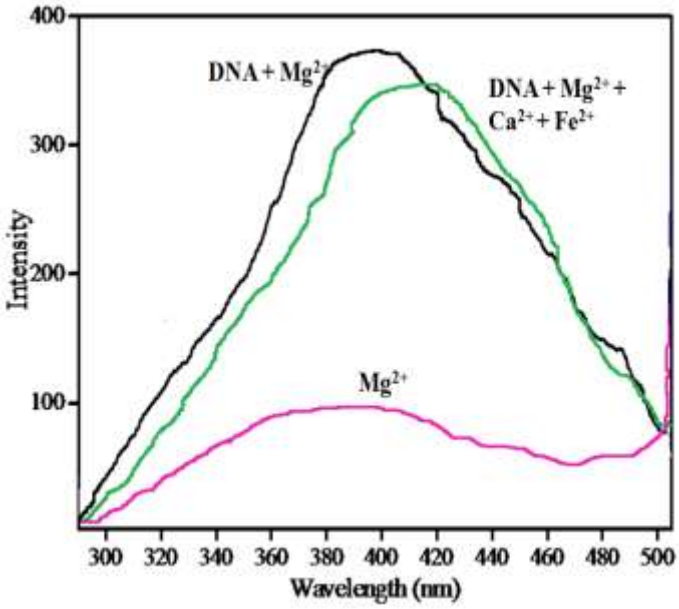

Figure 20 Fluorescence spectra of Mg^{+} ion with and without DNA

From the figure 20, it was tried to determine whether DNA could detect Mg^{2+} ions in the presence of other two metal ions. The fluorescence intensity of DNA with combination of all three metal ions and DNA with only Mg^{2+} ions were approximately same. So it was almost proved that the system could detect Mg^{2+} ion.

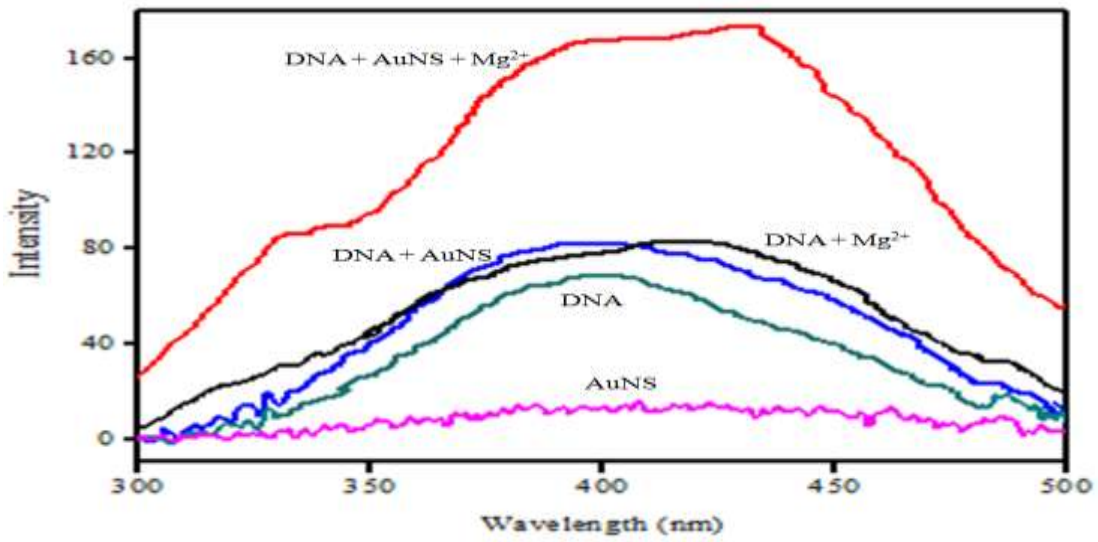

Figure 21. Fluorescence spectra of DNA-AuNS with and without Mg^{2+} ions

To evaluate the interaction of DNA-Gold nanoparticles with Mg^{2+} ion, DNA-Gold nanospheres were mixed with different concentrations of Mg^{2+} ions. Figure 21 shows the

fluorescence emission spectra of DNA-Gold nanospheres as an indicator of presence of Mg^{2+} ion. The fluorescence intensity gradually increases as the Mg^{2+} ion concentration increases (Liu et al. 2007).

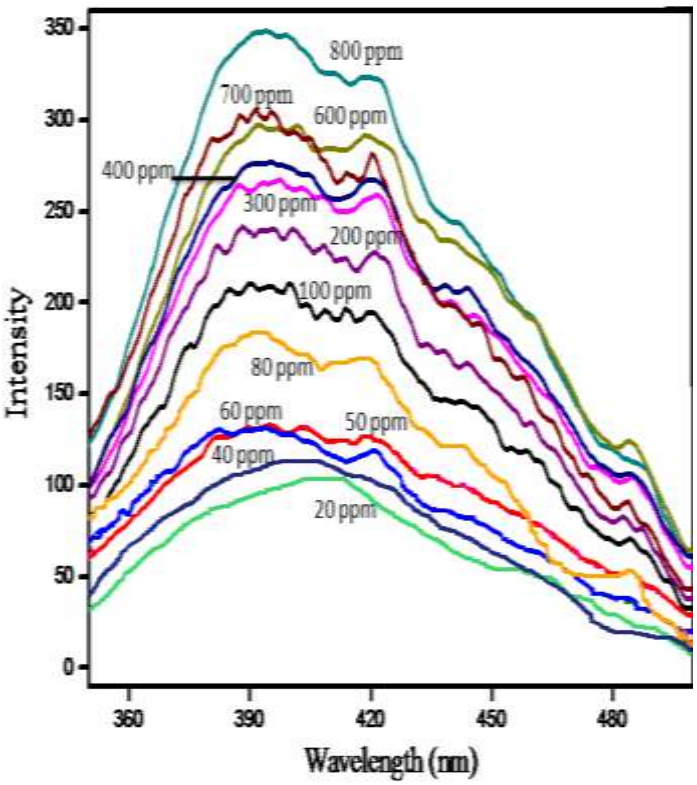

Figure 22. Increase in intensity with increasing concentration of Mg^{2+} ions

In figure 22, the fluorescence activity of the DNA-Gold nanospheres was monitored over a range of ion concentration to evaluate the lowest concentration at which Mg^{2+} ions could be detected. For detection of Mg^{2+} ions, concentration of Mg^{2+} ions varying from 20 to 800 ppm were added to a solution of DNA-Gold nanoparticles (100 µL) to obtain the limit of detection and metal ions response range of the DNA-Gold nanospheres. After 15 min incubation, the changes in fluorescence behavior of Mg^{2+} treated solution were observed using fluorescence spectrometer.

Standard Graph:

As shown in figure 23, a graph was plotted using the values obtained from fluorescence intensity graph given in figure 22. It was observed that on increasing the concentration of Mg^{2+} ions above 100 ppm, the graph become uneven. The graph was plotted from 20 ppm to 800 ppm Mg^{2+} ion concentration but from the plot, the straight line was obtained only from 20 to 100 ppm and above this concentration, the line was not following any pattern.

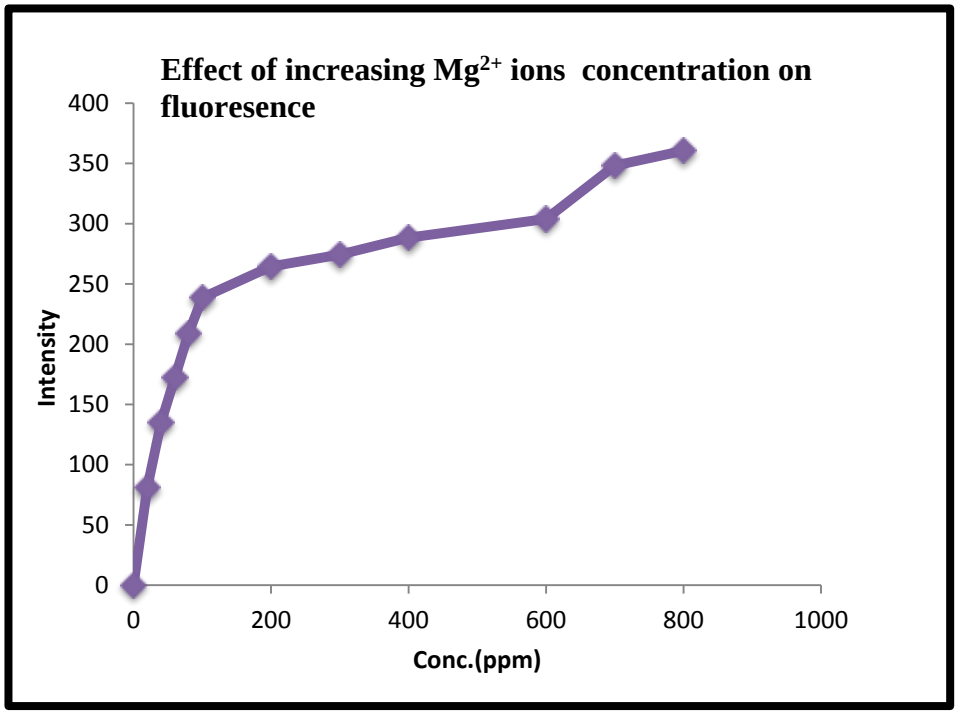

Figure 23. Graph of Change in fluorescence with increase in Mg^{2+} ion concentration

It can be stated from the graph of figure 23 that DNA-Gold nanocomposites which were used as sensor for magnesium ions were only effective up to 100 ppm. On further increasing the concentration of Mg^{2+} ions, the linearity of graph was lost and its predictability was decreased.

In figure 24, the standard curve was plotted up to 100 ppm of Mg^{2+} ion concentration in which direct effect of increase in concentration was clearly shown as intensity also increased.

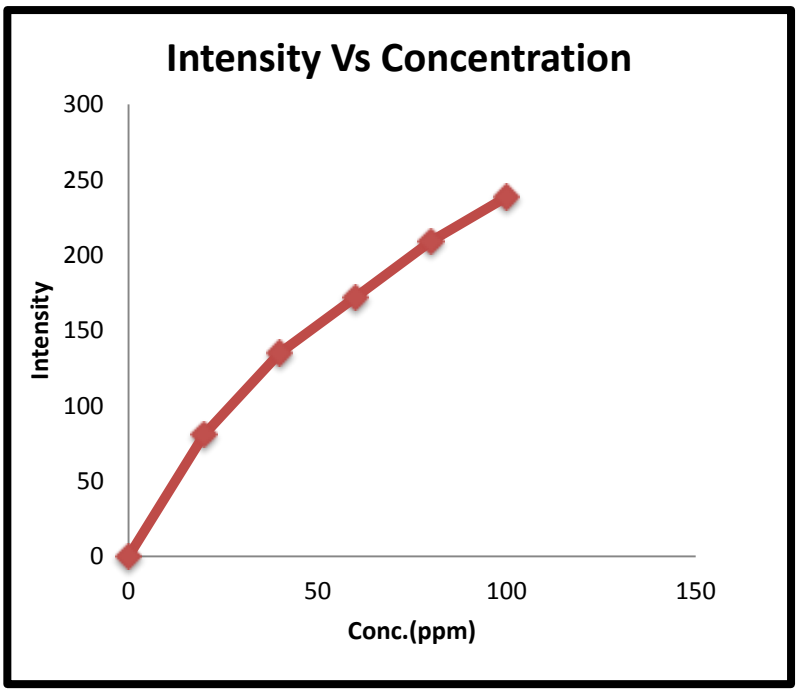

Figure 24. Standard curve of Intensity Vs Concentration

This standard plot of figure 24 was used to determine the concentration of magnesium in the given samples to confirm the importance of DNA-Gold nanoparticles as a detector.

Analysis of real life samples:

To analyze the activity of DNA-AuNS, this system was used to detect magnesium ions in different samples. Laboratory tap water and Gelusil (antacid) were taken for analysis. For the detection procedure, sample was prepared and protocol for detection was similar to that elaborated above for Mg^{2+} ions concentration detection. Some samples with unknown concentration were also used to check the viability of this sensing process. From figure 25, the fluorescence intensity of Gelusil was 900 a.u and from the standard curve, we know that there is fluorescence of 238 a.u for 100 ppm concentration of Mg^{2+} ions. Hence, by using this relationship between intensity and concentration, we calculated the concentration of Mg^{2+} ion in Gelusil which was 360 ppm but 300 ppm was mentioned on its cover (Li et al. 2010). This slight variation might be due to the presence of other interfering ions present in the medicine. In the case of tap water, the concentration was not known so by using DNA-Gold nanoparticles detection system we get to know the amount of magnesium present in the water. It was obtained as 52 ppm by converting the intensity into concentration using values of standard graph.

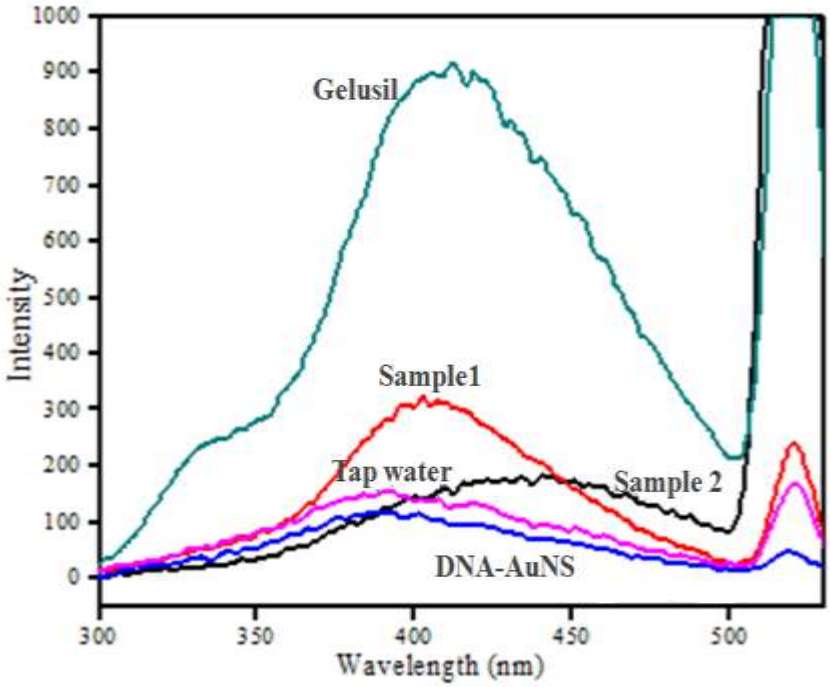

Figure 25. Fluorescence spectra of real life samples

After the fluorescence intensity testing of the above mentioned samples, the results were summarized in Table 3.

Table 3. Determination of Mg^{2+} ion concentration

S.No	Sample	Intensity	Mg^{2+} ions Conc.(ppm) obtained from standard graph	Real concentration (ppm) of Mg^{2+} ions
1.	Gelusil	900 a.u	360	300
2.	Tap water	150 a.u	52	--
3.	Sample 1	180 a.u	62	50
4.	Sample 2	310 a.u	120	150

From Table 3, it was analyzed that the concentration value obtained from standard curve is almost similar to their real value.

Sample 1 and sample 2 were the two samples, used to cross check our detection system. In both samples, known amount of Mg^{2+} ions were added in the water and then their fluorescence intensity were measured. In sample 1, 60 ppm of Mg^{2+} ions were added and through fluorescence the concentration obtained were 80 ppm and for sample 2, 150 ppm Mg^{2+} ions were added and 120 ppm was obtained through standard curve.

Hence, to large extend this novel sensing system is reliable for detection of magnesium ions. It is simple and can be easily carried out by simple mixing and incubation of the sample at room temperature. Because of its simplicity, rapidity and sensitivity, the DNA–Gold nanocomposites sensing system demonstrated here can prove to be a powerful sensor in near future.

8. Conclusion

This study deals with the development of DNA-Gold nanocomposites and their characterization through various techniques. Many unique properties of this hybrid nanomaterial are attributed to the DNA molecule. One of these properties is the fluorescence intensity. The fluorescence intensity of DNA increases when DNA binds with AuNS. Using this property, they were used as metal ion detection system. This system detected the concentration of Mg^{2+} ions in the solutions. This sensing system is considered to be very sensitive with a limit of detection from 20 ppm to 800 ppm for Mg^{2+} ions. The fluorescence intensity of DNA-AuNP was remarkably specific for Mg^{2+} ions in the presence of other metal ions and therefore, it can be used in various environmental and industrial monitoring applications. The DNA-Gold nanocomposites sensing system described in this study holds future promise in investigating the presence of many metal ions.

9. References

Abdelhalim, M. A. K.; Mady, M. M.; Ghannam, M. M. Physical Properties of Different Gold Nanoparticles: Ultraviolet-Visible and Fluorescence Measurements. *J Nanomed Nanotechol*, **2012**, 3(3), 100-133

Bacalocostantis, I.; Mane, V. P.; Kang, M. S.; Goodley, A. S.; Muro, S.; Kofinas, P. Effect of Thiol Pendant Conjugates on Plasmid DNA Binding, Release, and Stability of Polymeric Delivery Vectors. *Biomacromolecules*, **2012,** 13(5), 1331-9

Brown, K. R.; Natan, M. J. Hydroxylamine Seeding of Colloidal Au Nanoparticles in Solution and on Surfaces. *Langmuir*, **1998,** 14, 726-728

Cao, X.; Ye, Y.; Liu, S. Gold nanoparticle-based signal amplification for biosensing. *Analytical Biochemistry*, **2011,** 417, 1–16

Chang, K.Y.; Varani, G**.** Nucleic acids structure and recognition. *Nat. Struct. Biol.* **1997**, 4, 854–858

Chen, Y.; Munechika, K.; Ginger, D. S. Dependence of Fluorescence Intensity on the Spectral Overlap between Fluorophores and Plasmon Resonant Single Silver Nanoparticles. *Nano letters*, **2007**, 7(3), 690-696

Cobley, C.M.; Skrabalak, S.E.; Campbell, D.J.; Xia, Y. Shape-controlled synthesis of silver nanoparticles for plasmonic and sensing applications. *Plasmonics*, **2009,** 4, 171-179

Edgar, J. A.; McDonagh, A. M.; Cortie, M. B. Formation of Gold Nanorods by a Stochastic "Popcorn" Mechanism. *ACS Nano*, **2012**, 6 (2), 1116–1125

Eom, M. S.; Lee, Y. S.; Han, M. S. A Gold Nanoparticles-Based Colorimetric Assay for DNA-Binding Molecules Using Non-Cross-Linking Aggregation *Bull. Korean Chem. Soc.* **2012**, 33(4), 1341

Fan, J. A., He, Y.; Bao, K.; Wu, C.; Bao, J.; Schade, N. B., Manoharan, V. N.; Shvets, G.; Nordlander, P.; Liu, D. R.; Capasso, F.DNA-Enabled Self-Assembly of Plasmonic Nanoclusters. *NanoLett*. **2011**, 11, 4859–4864

Frank-Kamenetskii, M.D. Biophysics of the DNA molecule *Physics Reports.* **1997**, 288(1), 13-60

Friedberg, E.C.; Walker, G.C.; Siede, W**.** DNA Repair and Mutagenesis. W. H. Freeman and Company, New York, **1995**

Ganguly, M.; Pal, A.; Negishi, Y.; Pal, T. Synthesis of Highly Fluorescent Silver Clusters on Gold (I) Surface. *Langmuir* **2013**, 29, 2033−2043

Goodman, C. M.; Chari, N. S.; Han, G.; Hong, R.; Ghosh, P.; Rotello, V.M. DNA-binding by Functionalized Gold Nanoparticles: Mechanism and Structural Requirements. *ChemBiol Drug Des*, **2006**, 67, 297–304

Guha, S.; Roy, S.; Banerjee, A. Fluorescent Au@Ag Core Shell Nanoparticles with Controlled Shell Thickness and HgII Sensing. *Langmuir*, **2011**, 27 (21), 13198–13205

Hegner, M.; Wagner, P.; Semenza, G. Immobilizing DNA on gold via thiol modification for atomic force microscopy imaging in buffer solutions. *FEBS Lett.*, **1993,** 336(3), 452-456

Huang, X.; El-Sayed, M. A. Gold nanoparticles: Optical properties and implementations in cancer diagnosis and photothermal therapy. *Journal of Advanced Research*, **2010,** 1, 13–28

Hurst, S. J.; Lytton-Jean, A. K. R.; Mirkin C. A. Maximizing DNA Loading on a Range of Gold Nanoparticle Sizes. *Anal Chem*., **2006**, 78(24), 8313–8318

Inagaki, T.; Hamm, R.N.; Arakawa, E.T. Optical and dielectric properties of DNA in the extreme ultraviolet. *The journal of chemical physics*, **1947**, 61, 10

Jana, N. R.; Gearheart, L.; Murphy, C. J. Wet Chemical Synthesis of High Aspect Ratio Cylindrical Gold Nanorods. *J. Phys. Chem.*, **2001,** 105, 4065-4067

Kaur, R.; Pal, B. Co-catalysis effect of different morphological facets of as prepared Ag nanostructures for the photocatalytic oxidation reaction by TiO_2 aqueous slurry. *Materials Chemistry and Physics*, **2013,** 143, 393-399

Khlebtsov, N. G.; Dykman, L. A. Optical properties and biomedical applications of plasmonic nanoparticles. *Journal of Quantitative Spectroscopy & Radiative Transfer*, **2010,** 111, 1–35

Kim, T.; Lee, C.-H.; Joo, S.-W.; Lee, K. Kinetics of gold nanoparticle aggregation: Experiments and modeling. *Journal of Colloid and Interface Science*, **2008,** 318, 238–243

Li, C.-Z.; Male, K. B.; Hrapovic, S.; Luong, J. H. T. Fluorescence properties of gold nanorods and their application for DNA biosensing. *Chem. Commun*. **2005**, 3924-3926

Li, F.; Zhang, H.; Dever, B.; Li, X.-F.; Le, X. C. Thermal Stability of DNA Functionalized Gold Nanoparticles. *Bioconjugate Chem.*, **2013**, 24 (11), 1790–1797

Li, K.; Zhao, X.; Hammer, B. K.; Du, S.; Chen, Y. Nanoparticles Inhibit DNA Replication by Binding to DNA: Modeling and Experimental Validation. *ACS Nano*, **2013**, 7 (11), 9664–9674

Li, X.-M.; Fu, P.-Y.; Liu, J.-M.; Zhang, S.-S. Biosensor for multiplex detection of two DNA target sequences using enzyme-functionalized Au nanoparticles as signal amplification. *AnalyticaChimicaActa*, **2010,** 673,133–138

Li, Z.; Niu, T.; Zhang, Z.; Feng, G.; Bi, S. Effect of monovalent cations (Li^+, Na^+, K^+, Cs^+) on self-assembly of thiol-modified double-stranded and single-stranded DNA on gold electrode. *Analyst*, **2012**, 137, 1680

Lia, Y.; Schluesenerb, H. J.; Xua, S. Gold nanoparticle-based biosensors. *Gold Bulletin*, **2010,** 43, 29-41

Liang, Z.; Zhang, J.; Wang, L.; Song, S.; Fan, C.; Li, G. A Centrifugation-based Method for Preparation of Gold Nanoparticles and its Application in Biodetection. *Int. J. Mol. Sci.*, **2007**, 8, 526-532

Liao, H.; Hafner, J. H. Gold Nanorod Bioconjugates. *Chem. Mater.*, **2005,** 17, 4636-4641

Lim, S.; Koo, O. K.; You, Y. S.; Lee, Y. E.; Kim, M.-S.; Chang, P.-S.; Kang, D. H.; Yu, J.-H.; Choi, Y. J.; Gunasekaran, S. Enhancing Nanoparticle-Based Visible Detection by Controlling the Extent of Aggregation. *Scientific Reports*, **2012,** 2, 456

Lin, Y.-W.; Liu, C.-W.; Chang, H.-T. DNA functionalized gold nanoparticles for bioanalysis. *Anal. Methods*, **2009**, 1, 14–24

Liu, C.; Yang, X.; Yuan, H.; Zhou, Z.; Xiao, D. Preparation of Silver Nanoparticle and Its Application to the Determination of *ct*-DNA. *Sensors*, **2007**, *7*, 708-718

Mirkin, C.A.; Letsinger, R.C; Storhoff, J.J. A DNA-based method for rationally assembling nanoparticles into macroscopic materials. *Nature*, vol. **1996,** 382, 607

Nakao, H.; Shiigi, H.; Yamamoto, Y.; Tokonami, S.; Nagaoka, T.; Sugiyama, S.; Ohtani, T. Highly Ordered Assemblies of Au Nanoparticles Organized on DNA. *Nano letters* **2003**, 3(10), 1391-1394

Olby, R.C. The Path to the Double Helix: The Discovery of DNA. Dover Publications, **1994**

Pal, S.; Deng, Z.; Wang, H.; Zou, S.; Liu, Y.; Yan, H. DNA Directed Self-Assembly of Anisotropic Plasmonic Nanostructures. *J. Am. Chem. Soc.*, **2011**, 133, 17606–17609

Park, S. Y.; Stroud, D. Structure Formation, Melting, and the Optical Properties of Gold/DNA Nanocomposites: Effects of Relaxation Time. *Physical Review B*, **2003**, 68, 224201

Park, S. Y.; Stroud, D. Theory of Melting and the Optical Properties of Gold/DNA Nanocomposites. *Physical Review B.* **2003,** 67, 212-17

Park, S. Y.; Stroud, D. Theory of the optical properties of a DNA-modified gold nanoparticle system. *Physical Review B* **2003,** 338, 353–356

P´erez-Juste, J.; Pastoriza-Santos, I.; Liz-Marz´an, L. M.; Mulvaney, P. Gold nanorods: Synthesis, characterization and applications. *Coordination Chemistry Reviews*, **2005,** 249, 1870–1901

Pérez-Rentero, S.; Grijalvo, S.; Ferreira, R.; Eritja, R. Synthesis of Oligonucleotides Carrying Thiol Groups Using a Simple Reagent Derived from Threoninol. *Molecules*, **2012**, *17*, 10026-10045

Prado-Gotor, R.; Grueso, E. A kinetic study of the interaction of DNA with gold nanoparticles: mechanistic aspects of the interaction. *Phys. Chem. Chem. Phys*., **2011**, 13, 1479–148

Rafael, P.-G.; Elia, G. A kinetic study of the interaction of DNA with gold nanoparticles: mechanistic aspects of the interaction. *Phys. Chem. Chem. Phys*. **2011**, 13, 1479–148

Sajanlal, P. R.; Sreeprasad, T. S.; Samal, A. K.; Pradeep, T. Anisotropic nanomaterials: structure, growth, assembly, and functions. *Nano Reviews*, **2011**, 2, 5883

Sandström, P.; Boncheva, M.; Åkerman, B. Nonspecific and Thiol-Specific Binding of DNA to Gold Nanoparticles. *Langmuir*, **2003,** 19, 7537-7543

Shamoo, Y. Single-stranded DNA-binding Proteins. *Encyclopedia of life sciences*, **2002**

Storhoff, J. J.; Elghanian, R.; Mucic, R. C.; Mirkin, C. A.; Letsinger,R. L. One-Pot Colorimetric Differentiation of Polynucleotides with Single Base Imperfections Using Gold Nanoparticle Probes. *J. Am. Chem. Soc.*, **1998,** *120*, 1959-1964

Storhoff, J. J.; Mirkin, C. A. Programmed Materials Synthesis with DNA. *Chem. Rev.* **1999,** 99, 1849-1862

Tsai, S.-W.; Liaw, J.-W.; Hsu, F.-Y.; Chen, Y.-Y.; Lyu, M.-J.; Yeh, M.-H. Surface-Modified Gold Nanoparticles with Folic Acid as Optical Probes for Cellular Imaging. *Sensors*, **2008**, *8*, 6660-6673

Wang, Y.; Aili, D.; Seleg, R.; Tay, Y.; Baltzer, L.; Zhangab, H.; Liedberg, B. Specific functionalization of CTAB stabilized anisotropic gold nanoparticles with polypeptides for folding-mediated self-assembly. *J. Mater. Chem*., **2012**, 22, 20368

Warner, M. G.; Hutchison, J, E. Linear assemblies of nanoparticles electrostatically organized on DNA scaffolds. *Nature Materials*, **2003,** 2, 272 – 277

Warner, M. G.; Reed, S.M.; Hutchison, J. E. Small, water-soluble, ligand-stabilized gold nanoparticles synthesized by interfacial ligand exchange reactions. *Chem.Mater.***2000,** 12, 3316-3320

Witten, K. G.; Bretschneider, J. C.; Eckert, T.; Richtering, W.; Simon, U. Assembly of DNA-functionalized gold nanoparticles studied by UV/Vis-spectroscopy and dynamic light scattering. *Phys. Chem. Chem. Phys.*, **2008**, 10, 1870-1875

Yang, D.-P.; Cui, D.-X. Advances and Prospects of Gold Nanorods. *Chem. Asian J.*, **2008**, 3, 2010 – 2022

Yang, J.; Lee, J.Y.; Deivaraj, T. C.; Too, H.-P. Single Stranded DNA Induced Assembly of Gold Nanoparticles. *Molecular Engineering of Biological and Chemical Systems (MEBCS)*, **2003**

Zhang, X.; Liu, B.; Dave, N.; Servos, M. R.; Liu, J. Instantaneous Attachment of an Ultrahigh Density of Nonthiolated DNA to Gold Nanoparticles and Its Applications. *Langmuir*, **2012**, 28, 17053−17060

Zhang, X.; Servos, M. R.; Liu, J. Fast pH-assisted functionalization of silver nanoparticles with monothiolated DNA. *Chem. Commun*., **2012**, 48, 10114–10116